Grasping

28. Grasping

Domenico Prattichizzo, Jeffrey C. Trinkle

This chapter introduces fundamental models of grasp analysis. The overall model is a coupling of models that define contact behavior with widely used models of rigid-body kinematics and dynamics. The contact model essentially boils down to the selection of components of contact force and moment that are transmitted through each contact. Mathematical properties of the complete model naturally give rise to five primary grasp types whose physical interpretations provide insight for grasp and manipulation planning.

After introducing the basic model and types of grasps, this chapter focuses on the most important grasp characteristic: complete restraint. A grasp with complete restraint prevents loss of contact and thus is very secure. Two primary restraint properties are *form closure* and *force closure*. A form closure grasp guarantees maintenance of contact as long as the links of the hand and the object are well approximated as rigid and as long as the joint actuators are sufficiently strong. As will be seen, the primary difference between form closure and force closure grasps is the latter's reliance on contact friction. This translates into

requiring fewer contacts to achieve force closure than form closure.

28.1 Background

Mechanical hands were developed to give robots the ability to grasp objects of varying geometric and physical properties. The first robotic hand designed for dexterous manipulation was the Salisbury hand [28.1]. It has three three-jointed fingers; enough to control all six degrees of freedom of an object and the grip pressure. The fundamental grasp modeling and analysis done by Salisbury provides a basis for grasp synthesis and dexterous manipulation research which continues today. Some of the most mature analysis techniques are embedded in the software *GraspIt!* [28.2]. *GraspIt!*

contains models for several robot hands and provides tools for grasp selection, dynamic grasp simulation, and visualization.

The goal of this chapter is to give a thorough understanding of the all-important grasp properties of form and force closure. This will be done through detailed derivations of grasp models and discussions of illustrative examples. For an in-depth historical perspective and a treasure-trove bibliography of papers addressing a wide range of topics in grasping, the reader is referred to [28.3].

28.2 Models and Definitions

A mathematical model of grasping must be capable of predicting the behavior of the hand and object under the various loading conditions that may arise during grasping. Generally, the most desirable behavior is grasp maintenance in the face of unknown disturbing forces and moments applied to the object. Typically these disturbances arise from inertia forces which become appreciable during high-speed manipulation or applied forces such as those due to gravity. Grasp maintenance means that the contact forces applied by the hand are such that they prevent contact separation and unwanted contact sliding. The special class of grasps that can be maintained for every possible disturbing load is known as closure grasps. Figure 28.1 shows the Salisbury hand [28.1, 4] executing a closure grasp of an object by wrapping its fingers around it and pressing the object against its palm. Formal definitions, analysis, and computational tests for closure will be presented in Sect. 28.5.

Figure 28.2 illustrates some of the main quantities that will be used to model grasping systems. Assume that the links of the hand and the object are rigid and that there is a unique, well-defined tangent plane at each contact point. Let $\{N\}$ represent a conveniently chosen inertial frame fixed in the workspace. The frame $\{B\}$ is fixed to the object with its origin defined relative to $\{N\}$ by the vector $\boldsymbol{p} \in \mathbb{R}^3$, where $\mathbb{R}^3$ denotes three-dimensional Euclidean space. A convenient choice for $\boldsymbol{p}$ is the center of mass of the object. The position of contact point i in $\{N\}$ is defined by the vector $\boldsymbol{c}_i \in \mathbb{R}^3$. At contact point i, we define a frame $\{C\}_i$, with axes $\{\hat{\boldsymbol{n}}_i, \hat{\boldsymbol{t}}_i, \hat{\boldsymbol{o}}_i\}$ ($\{C\}_i$ is shown in *exploded* view). The unit vector $\hat{\boldsymbol{n}}_i$ contains $\boldsymbol{c}_i$ is normal to the contact tangent
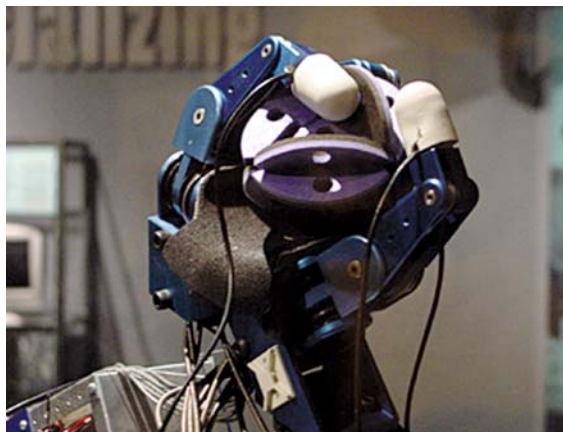
plane, and is directed toward the object. The other two unit vectors are orthogonal and lie in the tangent plane of the contact.

Let the joints be numbered from 1 to n_q. Denote by $\boldsymbol{q} = [q_1 \cdots q_{n_q}]^\top \in \mathbb{R}^{n_q}$ the vector of joint displacements, where the superscript $^\top$ indicates matrix transposition. Also, let $\boldsymbol{\tau} = [\tau_1 \cdots \tau_{n_q}]^\top \in \mathbb{R}^{n_q}$ represent joint loads (forces in prismatic joints and torques in revolute joints). These loads can result from actuator actions, other applied forces, and inertia forces. They could also arise from contacts between the object and hand. However, it will be convenient to separate joint loads into two components: those arising from contacts and those arising from all other sources. Throughout this chapter, noncontact loads will be denoted by $\boldsymbol{\tau}$.

Let $\boldsymbol{u} \in \mathbb{R}^{n_u}$ denote the vector describing the position and orientation of $\{B\}$ relative to $\{N\}$. For planar systems $n_u = 3$. For spatial systems, n_u is three plus the number of parameters used to represent orientation, typically three (for Euler angles) or four (for unit quaternions). Denote by $\boldsymbol{v} = [\boldsymbol{v}^\top \boldsymbol{\omega}^\top]^\top \in \mathbb{R}^{n_v}$ the twist of the object described in $\{N\}$. It is composed of the translational velocity $\boldsymbol{v} \in \mathbb{R}^3$ of the point $\boldsymbol{p}$ and the angular velocity $\boldsymbol{\omega} \in \mathbb{R}^3$ of the object, both expressed in $\{N\}$. A twist of a rigid body can be referred to any convenient frame fixed to the body. The components of the referred twist represent the velocity of the origin of the new frame and the angular velocity of the body, both expressed in the new frame. For a rigorous treatment of twists and
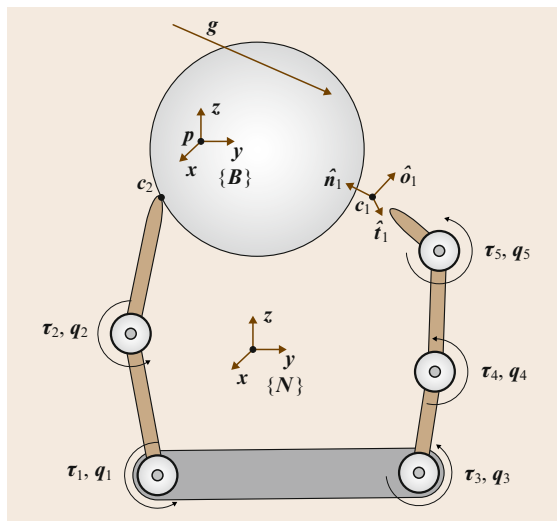

Fig. 28.1 The Salisbury hand grasping an object

Fig. 28.2 Main quantities for grasp analysis

wrenches see [28.5, 6]. Note that for planar systems, $v \in \mathbb{R}^2$ and $\omega \in \mathbb{R}$, and so $n_v = 3$.

Another important point is $\dot{u} \neq v$. Instead, these variables are related by the matrix V as:

$$\dot{u} = Vv , \qquad (28.1)$$

where the matrix $V \in \mathbb{R}^{n_u \times n_v}$ is not generally square but nonetheless satisfies $V^\top V = I$ [28.7], I is the identity matrix, and the dot over the u implies differentiation with respect to time. Note that, for planar systems, $V = I \in \mathbb{R}^{3 \times 3}$.

Let $f \in \mathbb{R}^3$ be the force applied to the object at the point p and let $m \in \mathbb{R}^3$ be the applied moment. These are combined into the object load, or wrench, vector denoted by $g = [f^\top m^\top]^\top \in \mathbb{R}^{n_v}$, where f and m are expressed in $\{N\}$. Like twists, wrenches can be referred to any convenient frame fixed to the body. One can think of this as translating the line of application of the force until it contains the origin of the new frame, then adjusting the moment component of the wrench to offset the moment induced by moving the line of the force. Last, the force and adjusted moment are expressed in the new frame. As done with the joint loads, the object wrench will be partitioned into two main parts: contact and noncontact wrenches. Throughout this chapter, g will denote the noncontact wrench on the object.

28.2.1 Velocity Kinematics

The material in this chapter is valid for a wide range of robot hands and other grasping mechanisms. The hand is assumed to be composed of a palm that serves as the common base for any number of fingers, each with any number of joints. The formulations given in this chapter are expressed explicitly in terms of only revolute and prismatic joints. However, most other common joints can be modeled by combinations of revolute and prismatic joints (e.g., cylindrical, spherical, and planar). Any number of contacts may occur between any link and the object.

Grasp Matrix and Hand Jacobian

Two matrices are of the utmost importance in grasp analysis: the *grasp matrix* G and the *hand Jacobian* J. These matrices define the relevant velocity kinematics and force transmission properties of the contacts. The following derivations of G and J will be done under the assumption that the system is three-dimensional. Changes for planar systems will be noted later.

Each contact should be considered as two coincident points: one on the hand and one on the object. The hand

Jacobian maps the joint velocities to the twists of the hand expressed in the contact frames, while the transpose of the grasp matrix refers the object twist to the contact frames. Finger joint motions induce a rigid-body motion in each link of the hand. It is implicit in the terminology, *twists of the hand*, that the twist referred to contact i is the twist of the link involved in contact i. Thus these matrices can be derived from the transforms that change the reference frame of a twist.

To derive the grasp matrix, let $\omega_{\text{obj}}^{\text{N}}$ denote the angular velocity of the object expressed in $\{N\}$ and let $v_{i,\text{obj}}^{\text{N}}$, also expressed in $\{N\}$, denote the velocity of the point on the object coincident with the origin of $\{C\}_i$. These velocities can be obtained from the object twist referred to $\{N\}$ as:

$$\begin{pmatrix} v_{i,\text{obj}}^{\text{N}} \\ \omega_{\text{obj}}^{\text{N}} \end{pmatrix} = P_i^\top v , \qquad (28.2)$$

where

$$P_i = \begin{pmatrix} I_{3 \times 3} & 0 \\ S(c_i - p) & I_{3 \times 3} \end{pmatrix} , \qquad (28.3)$$

$I_{3 \times 3} \in \mathbb{R}^{3 \times 3}$ is the identity matrix, and $S(c_i - p)$ is the cross-product matrix, that is, given a three-vector $r = [r_x r_y r_z]^\top$, $S(r)$ is defined as:

$$S(r) = \begin{pmatrix} 0 & -r_z & r_y \\ r_z & 0 & -r_x \\ -r_y & r_x & 0 \end{pmatrix} .$$

The object twist referred to $\{C\}_i$ is simply the vector on the left-hand side of (28.2) expressed in $\{C\}_i$. Let $R_i = [\hat{n}_i \, \hat{t}_i \, \hat{o}_i] \in \mathbb{R}^{3 \times 3}$ represent the orientation of the i-th contact frame $\{C\}_i$ with respect to the inertial frame (the unit vectors $\hat{n}_i$, $\hat{t}_i$, and $\hat{o}_i$ are expressed in $\{N\}$). Then the object twist referred to $\{C\}_i$ is given as:

$$v_{i,\text{obj}} = \overline{R}_i^\top \begin{pmatrix} v_{i,\text{obj}}^{\text{N}} \\ \omega_{\text{obj}}^{\text{N}} \end{pmatrix} , \qquad (28.4)$$

where $\overline{R}_i = \text{Blockdiag}(R_i, R_i) = \begin{pmatrix} R_i & 0 \\ 0 & R_i \end{pmatrix} \in \mathbb{R}^{6 \times 6}$.

Substituting $P_i^\top v$ from (28.2) into (28.4) yields the partial grasp matrix $\tilde{G}_i^\top \in \mathbb{R}^{6 \times 6}$, which maps the object twist from $\{N\}$ to $\{C\}_i$:

$$v_{i,\text{obj}} = \tilde{G}_i^\top v , \qquad (28.5)$$

where

$$\tilde{G}_i^\top = \overline{R}_i^\top P_i^\top . \qquad (28.6)$$

The hand Jacobian can be derived similarly. Let $\omega_{i,\text{hnd}}^{N}$ be the angular velocity of the link of the hand touching the object at contact i, expressed in $\{N\}$, and define $v_{i,\text{hnd}}^{N}$ as the translational velocity of contact i on the hand, expressed in $\{N\}$. These velocities are related to the joint velocities through the matrix Z_i whose columns are the Plücker coordinates of the axes of the joints [28.5, 6]. We have:

$$\begin{pmatrix} v_{i,\text{hnd}}^{N} \\ \omega_{i,\text{hnd}}^{N} \end{pmatrix} = Z_i \dot{q} \; , \tag{28.7}$$

where $Z_i \in \mathbb{R}^{6 \times n_q}$ is defined as:

$$Z_i = \begin{pmatrix} d_{i,1} & \cdots & d_{i,n_q} \\ l_{i,1} & \cdots & l_{i,n_q} \end{pmatrix} \; , \tag{28.8}$$

with the vectors $d_{i,j}, l_{i,j} \in \mathbb{R}^3$ defined as:

$$d_{i,j} = \begin{cases} \mathbf{0}_{3\times 1} & \text{if contact } i \text{ does} \\ & \text{not affect joint } j \; , \\ \hat{z}_j & \text{if joint } j \text{ is prismatic} \; , \\ S(c_i - \zeta_j)^{\top} \hat{z}_j & \text{if joint } j \text{ is revolute} \; , \end{cases}$$

$$l_{i,j} = \begin{cases} \mathbf{0}_{3\times 1} & \text{if contact } i \text{ does} \\ & \text{not affect joint } j \; , \\ \mathbf{0}_{3\times 1} & \text{if joint } j \text{ is prismatic} \; , \\ \hat{z}_j & \text{if joint } j \text{ is revolute} \; , \end{cases}$$

where ζ_j is the origin of the coordinate frame associated with the j-th joint and $\hat{z}_j$ is the unit vector in the direction of the z-axis in the same frame, as shown in Fig. 28.11. Both vectors are expressed in $\{N\}$. These frames may be assigned by any convenient method, for example, the Denavit–Hartenberg method [28.8]. The $\hat{z}_j$-axis is the rotational axis for revolute joints and the direction of translation for prismatic joints.

The final step in referring the hand twists to the contact frames is to change the frame of expression of $v_{i,\text{hnd}}^{N}$ and $\omega_{i,\text{hnd}}^{N}$ to $\{C\}_i$:

$$v_{i,\text{hnd}} = \overline{R}_i^{\top} \begin{pmatrix} v_{i,\text{hnd}}^{N} \\ \omega_{i,\text{hnd}}^{N} \end{pmatrix} \; . \tag{28.9}$$

Combining (28.9) and (28.7) yields the partial hand Jacobian $\tilde{J}_i \in \mathbb{R}^{6 \times n_q}$, which relates the joint velocities to the contact twists on the hand:

$$v_{i,\text{hnd}} = \tilde{J}_i \dot{q} \; , \tag{28.10}$$

where

$$\tilde{J}_i = \overline{R}_i^{\top} Z_i \; . \tag{28.11}$$

To compact notation, stack all the twists of the hand and object into the vectors $v_{c,\text{hnd}} \in \mathbb{R}^{6n_c}$ and $v_{c,\text{obj}} \in \mathbb{R}^{6n_c}$ as follows:

$$v_{c,\xi} = \left(v_{1,\xi}^{\top} \;\; \cdots \;\; v_{n_c,\xi}^{\top} \right)^{\top} \; , \quad \xi = \{\text{obj}, \text{hnd}\} \; .$$

Now the *complete grasp matrix* $\tilde{G} \in \mathbb{R}^{6 \times 6n_c}$ and the *complete hand Jacobian* $\tilde{J} \in \mathbb{R}^{6n_c \times n_q}$ relate the various velocity quantities as

$$v_{c,\text{obj}} = \tilde{G}^{\top} v \; , \tag{28.12}$$

$$v_{c,\text{hnd}} = \tilde{J} \dot{q} \; , \tag{28.13}$$

where

$$\tilde{G}^{\top} = \begin{pmatrix} \tilde{G}_1^{\top} \\ \vdots \\ \tilde{G}_{n_c}^{\top} \end{pmatrix} \; , \quad \tilde{J} = \begin{pmatrix} \tilde{J}_1 \\ \vdots \\ \tilde{J}_{n_c} \end{pmatrix} \; . \tag{28.14}$$

The term *complete* is used to emphasize that all $6n_c$ twist components at the contacts are included in the mapping. See Example 1, Part 1 and Example 3, Part 1 at the end of this chapter for clarification.

Contact Modeling

Three contact models useful for grasp analysis are reviewed here. For a complete discussion of contact modeling in robotics, readers are referred to Chap. 27.

The three models of greatest interest in grasp analysis are known as *point contact without friction*, *hard finger*, and *soft finger* [28.9]. These models select components of the contact twists to transmit between the hand and the object. This is done by equating a subset of the components of the hand and object twist at each contact. The corresponding components of the contact force and moment are also equated, but without regard for the constraints imposed by contact unilaterality and friction models (Sect. 28.5.2).

The point-contact-without-friction (PwoF) model is used when the contact patch is very small and the surfaces of the hand and object are slippery. With this model, only the normal component of the translational velocity of the contact point on the hand (i. e., the first component of $v_{i,\text{hnd}}$) is transmitted to the object. The two components of tangential velocity and the three components of angular velocity are not transmitted. Analogously, the normal component of the contact force is transmitted, but the frictional forces and moments are assumed to be negligible.

Table 28.1 Primary notation for grasp analysis

Notation	Definition
n_c	number of contacts
n_q	number of joints of hand
n_v	number of degrees of freedom of object
$\boldsymbol{q} \in \mathbb{R}^{n_q}$	joint displacements
$\dot{\boldsymbol{q}} \in \mathbb{R}^{n_q}$	joint velocities
$\boldsymbol{\tau} \in \mathbb{R}^{n_q}$	noncontact joint loads
$\boldsymbol{u} \in \mathbb{R}^{n_u}$	position and orientation of object
$\boldsymbol{v} \in \mathbb{R}^{n_v}$	twist of object
$\boldsymbol{g} \in \mathbb{R}^{n_v}$	noncontact object wrench
$\{\boldsymbol{B}\}$	frame fixed in object
$\{\boldsymbol{C}\}_i$	frame at contact i
$\{\boldsymbol{N}\}$	inertial frame

Table 28.2 Selection matrices for three contact models

Model	ℓ_i	$\boldsymbol{H}_{i\mathrm{F}}$	$\boldsymbol{H}_{i\mathrm{M}}$
PwoF	1	$\begin{pmatrix} 1 & 0 & 0 \end{pmatrix}$	vacuous
HF	3	$\mathbf{I}_{3\times3}$	vacuous
SF	4	$\mathbf{I}_{3\times3}$	$\begin{pmatrix} 1 & 0 & 0 \end{pmatrix}$

A hard-finger (HF) model is used when there is significant contact friction, but the contact patch is small, so that no appreciable friction moment exists. When this model is applied to a contact, all three translational velocity components of the contact point on the hand (i. e., the first three components of $\boldsymbol{v}_{i,\mathrm{hnd}}$) and all three components of the contact force are transmitted through the contact. None of the angular velocity components or moment components are transmitted.

The soft-finger (SF) model is used in situations in which the surface friction and the contact patch are large enough to generate significant friction forces and a friction moment about the contact normal. At a contact where this model is enforced, the three translational velocity components of the contact on the hand and the angular velocity component about the contact normal are transmitted (i. e., the first four components of $\boldsymbol{v}_{i,\mathrm{hnd}}$). Similarly, all three components of contact force and the normal component of the contact moment are transmitted.

Remark. The reader may see a contradiction between the rigid-body assumption and the soft-finger model. The rigid-body assumption is an approximation that simplifies all aspects of the analysis of grasping, but nonetheless it is sufficiently accurate in many real situations and grasp analysis would be impractical without. On the other hand, the need for a soft-finger model is a clear admission that the finger links and object are not rigid. However, it can be usefully applied in situations in which the amount of deformation required to obtain a large contact patch is small. Such situations occur when the local surface geometries are similar. If large finger or body deformations exist in the real sys-

tem, the rigid-body approach presented in this chapter should be used with caution.

To develop the PwoF, HF, and SF models, define the relative twist at contact i as:

$$\begin{pmatrix} \tilde{\boldsymbol{J}}_i & -\tilde{\boldsymbol{G}}_i^\top \end{pmatrix} \begin{pmatrix} \dot{\boldsymbol{q}} \\ \boldsymbol{v} \end{pmatrix} = \boldsymbol{v}_{i,\mathrm{hnd}} - \boldsymbol{v}_{i,\mathrm{obj}} \ .$$

A particular contact model is defined through the matrix $\boldsymbol{H}_i \in \mathbb{R}^{\ell_i \times 6}$, which selects ℓ_i components of the relative contact twist and sets them to zero:

$$\boldsymbol{H}_i(\boldsymbol{v}_{i,\mathrm{hnd}} - \boldsymbol{v}_{i,\mathrm{obj}}) = \boldsymbol{0} \ .$$

These components are referred to as transmitted degrees of freedom (DOF). Define $\boldsymbol{H}_i$ as:

$$\boldsymbol{H}_i = \begin{bmatrix} \boldsymbol{H}_{i\mathrm{F}} & \boldsymbol{0} \\ \boldsymbol{0} & \boldsymbol{H}_{i\mathrm{M}} \end{bmatrix} , \tag{28.15}$$

where $\boldsymbol{H}_{i\mathrm{F}}$ and $\boldsymbol{H}_{i\mathrm{M}}$ are the translational and rotational component selection matrices, respectively. Table 28.2 gives the definitions of the selection matrices for the three contact models, where *vacuous* means that the corresponding block row matrix in (28.15) is void (i. e., it has zero rows and columns). Notice that, for the SF model, $\boldsymbol{H}_{i\mathrm{M}}$ selects rotation about the contact normal.

After choosing a transmission model for each contact, the contact constraint equations for all n_c contacts can be written in compact form as:

$$\boldsymbol{H}(\boldsymbol{v}_{c,\mathrm{hnd}} - \boldsymbol{v}_{c,\mathrm{obj}}) = \boldsymbol{0} \ , \tag{28.16}$$

where

$$\boldsymbol{H} = \mathrm{Blockdiag}(\boldsymbol{H}_1, \dots, \boldsymbol{H}_{n_c}) \in \mathbb{R}^{\ell \times 6 n_c} \ ,$$

and the number of twist components ℓ transmitted through the n_c contacts is given by $\ell = \sum_{i=1}^{n_c} \ell_i$.

Finally, by substituting (28.12) and (28.13) into (28.16) one obtains:

$$\begin{pmatrix} \boldsymbol{J} & -\boldsymbol{G}^\top \end{pmatrix} \begin{pmatrix} \dot{\boldsymbol{q}} \\ \boldsymbol{v} \end{pmatrix} = \boldsymbol{0} \ , \tag{28.17}$$

where the grasp matrix and hand Jacobian are

$$\boldsymbol{G}^\top = \boldsymbol{H}\tilde{\boldsymbol{G}}^\top \in \mathbb{R}^{\ell \times 6} \ ,$$
$$\boldsymbol{J} = \boldsymbol{H}\tilde{\boldsymbol{J}} \in \mathbb{R}^{\ell \times n_q} \ . \tag{28.18}$$

Part D | 28.2

Table 28.3 Selection matrices for planar contact models

Model	ℓ_i	H_{iF}	H_{iM}
PwoF	1	$\begin{pmatrix} 1 & 0 \end{pmatrix}$	vacuous
HF/SF	2	$I_{2\times 2}$	vacuous

For more details on the construction of H, the grasp matrix, and the hand Jacobian, readers are referred to [28.10–12] and the references therein.

See Example 1, Part 2 and Example 3, Part 2.

It is worth noting that (28.17) can be written in the following form:

$$J\dot{q} = v_{cc,\text{hnd}} = v_{cc,\text{obj}} = G^\top v , \tag{28.19}$$

where $v_{cc,\text{hnd}}$ and $v_{cc,\text{obj}}$ contain only the components of the twists that are transmitted by the contacts. Note that this equation implies that grasp *maintenance* is defined as the situation in which all these equations are maintained over time. Thus, when a contact is frictionless, contact maintenance implies continued contact, but sliding is allowed. However, when a contact is of the HF type, contact maintenance implies sticking contact, since sliding would violate the HF model. Similarly, for an SF contact, there may be no sliding or relative rotation about the contact normal.

For the remainder of this chapter, it will be assumed that $v_{cc,\text{hnd}} = v_{cc,\text{obj}}$, so the notation will be shortened to v_{cc}.

Planar Simplifications

Assume that the plane of motion is the (x, y)-plane of $\{N\}$. The vectors v and g reduce in dimension from six to three by dropping components three, four, and five. The dimensions of the vectors c_i and p reduce from three to two. The i-th rotation matrix becomes $R_i = \left(\hat{n}_i \, \hat{t}_i\right) \in \mathbb{R}^{2\times 2}$ (where the third components of $\hat{n}_i$ and $\hat{t}_i$ are dropped) and (28.4) holds with $\overline{R}_i = \text{Blockdiag}(R_i, 1) \in \mathbb{R}^{3\times 3}$. Equation (28.2) holds with:

$$P_i = \begin{pmatrix} I_{2\times 2} & 0 \\ S_2(c_i - p) & 1 \end{pmatrix} ,$$

where S_2 is the analog of the cross-product matrix for two-dimensional vectors, given as

$$S_2(r) = \begin{pmatrix} -r_y & r_x \end{pmatrix} .$$

Table 28.4 Vectors of contact force and moment components, also known as the wrench intensity vector, transmitted through contact i

Model	λ_i
PwoF	(f_{in})
HF	$\left(f_{\text{in}} \, f_{\text{it}} \, f_{\text{io}} \right)^\top$
SF	$\left(f_{\text{in}} \, f_{\text{it}} \, f_{\text{io}} \, m_{\text{in}} \right)^\top$

Equation (28.7) holds with $d_{i,j} \in \mathbb{R}^2$ and $l_{i,j} \in \mathbb{R}$ defined as

$$d_{i,j} = \begin{cases} \mathbf{0}_{2\times 1} & \text{if contact force } i \text{ does} \\ & \text{not affect the joint } j , \\ \hat{z}_j & \text{if joint } j \text{ is prismatic ,} \\ S(c_i - \zeta_j)^\top & \text{if joint } j \text{ is revolute ,} \end{cases}$$

$$l_{i,j} = \begin{cases} 0 & \text{if contact force } i \text{ does} \\ & \text{not affect joint } j , \\ 0 & \text{if joint } j \text{ is prismatic ,} \\ 1 & \text{if joint } j \text{ is revolute .} \end{cases}$$

The complete grasp matrix and hand Jacobian have reduced sizes: $\tilde{G}^\top \in \mathbb{R}^{3n_c \times 3}$ and $\tilde{J} \in \mathbb{R}^{3n_c \times n_q}$.

As far as contact constraint is concerned, (28.15) holds with H_{iF} and H_{iM} in Table 28.3.

In planar cases, the SF and HF models are equivalent, because the object and the hand lie in a plane. Rotations about the contact normals would cause out-of-plane motions. Finally, the dimensions of the grasp matrix and hand Jacobian are reduced to the following sizes: $G^\top \in \mathbb{R}^{\ell \times 3}$ and $J \in \mathbb{R}^{\ell \times n_q}$. See Example 1, Part 3 and Example 2, Part 1.

28.2.2 Dynamics and Equilibrium

The dynamic equations of the system can be written as:

$$M_{\text{hnd}}(q)\ddot{q} + b_{\text{hnd}}(q, \dot{q}) + J^\top \lambda = \tau_{\text{app}}$$
$$M_{\text{obj}}(u)\dot{v} + b_{\text{obj}}(u, v) - G\lambda = g_{\text{app}}$$
$$\text{subject to constraint (28.17) ,} \tag{28.20}$$

where $M_{\text{hnd}}(\cdot)$ and $M_{\text{obj}}(\cdot)$ are symmetric positive-definite inertia matrices and $b_{\text{hnd}}(\cdot, \cdot)$ and $b_{\text{obj}}(\cdot, \cdot)$ are the velocity-product terms, g_{app} is the force and moment applied to the object by gravity and other external sources, τ_{app} is the vector of external loads and actuator actions, and the vector $G\lambda$ is the total

wrench applied to the object by the hand. The vector $\boldsymbol{\lambda}$ contains the contact force and moment components transmitted through the contacts and expressed in the contact frames. Specifically, $\boldsymbol{\lambda} = [\boldsymbol{\lambda}_1^\top \cdots \boldsymbol{\lambda}_{n_c}^\top]^\top$, where $\boldsymbol{\lambda}_i = \boldsymbol{H}_i[f_{\text{in}}\ f_{it}\ f_{io}\ m_{\text{in}}\ m_{it}\ m_{io}]^\top$. The subscripts indicate one normal (n) and two tangential (t, o) components of contact force $\boldsymbol{f}$ and moment $\boldsymbol{m}$. For an SF, HF, or PwoF contact, $\boldsymbol{\lambda}_i$ is defined as in Table 28.4. Finally, it is worth noting that $\boldsymbol{G}_i\boldsymbol{\lambda}_i = \tilde{\boldsymbol{G}}_i\boldsymbol{H}_i\boldsymbol{\lambda}_i$ is the wrench applied through contact i, where $\tilde{\boldsymbol{G}}_i$ and $\boldsymbol{H}_i$ are defined in (28.6) and (28.15). The vector $\boldsymbol{\lambda}_i$ is known as the wrench intensity vector for contact i.

Equation (28.20) represents the dynamics of the hand and object without regard for the kinematic constraints imposed by the contact models. Enforcing them, the dynamic model of the system can be written as:

$$\begin{pmatrix} \boldsymbol{J}^\top \\ -\boldsymbol{G} \end{pmatrix} \boldsymbol{\lambda} = \begin{pmatrix} \boldsymbol{\tau} \\ \boldsymbol{g} \end{pmatrix} \tag{28.21}$$

subject to $\boldsymbol{J}\dot{\boldsymbol{q}} = \boldsymbol{G}^\top \boldsymbol{v} = \boldsymbol{v}_{cc}$, where

$$\boldsymbol{\tau} = \boldsymbol{\tau}_{\text{app}} - \boldsymbol{M}_{\text{hnd}}(\boldsymbol{q})\ddot{\boldsymbol{q}} - \boldsymbol{b}_{\text{hnd}}(\boldsymbol{q}, \dot{\boldsymbol{q}}),$$
$$\boldsymbol{g} = \boldsymbol{g}_{\text{app}} - \boldsymbol{M}_{\text{obj}}(\boldsymbol{u})\dot{\boldsymbol{v}} - \boldsymbol{b}_{\text{obj}}(\boldsymbol{u}, \boldsymbol{v}). \tag{28.22}$$

One should notice that the dynamic equations are closely related to the kinematic model in (28.17). Specifically, just as $\boldsymbol{J}$ and $\boldsymbol{G}^\top$ transmit only selected

components of contact twists, $\boldsymbol{J}^\top$ and $\boldsymbol{G}$ in (28.20) serve to transmit only the corresponding components of the contact wrenches.

When the inertia terms are negligible, as occurs during slow motion, the system is said to be quasistatic. In this case, (28.22) becomes:

$$\boldsymbol{\tau} = \boldsymbol{\tau}_{\text{app}},$$
$$\boldsymbol{g} = \boldsymbol{g}_{\text{app}}, \tag{28.23}$$

and does not depend on joint and object velocities. Consequently, when the grasp is in static equilibrium or moves quasistatically, one can solve the first equation and the constraint in (28.21) independently to compute $\boldsymbol{\lambda}$, $\dot{\boldsymbol{q}}$, and $\boldsymbol{v}$. It is worth noting that such a force/velocity decoupled solution is not possible when dynamic effects are appreciable, since the first equation in (28.21) depends on the third one through (28.22).

Remark. Equation (28.21) highlights an important alternative view of the grasp matrix and the hand Jacobian. $\boldsymbol{G}$ can be thought of as a mapping from the transmitted contact forces and moments to the set wrenches that the hand can apply to the object, while $\boldsymbol{J}^\top$ can be thought of as a mapping from the transmitted contact forces and moments to the vector of joint loads. Notice that these interpretations hold for both dynamic and quasistatic conditions.

28.3 Controllable Twists and Wrenches

In hand design and in grasp and manipulation planning, it is important to know the set of twists that can be imparted to the object by movements of the fingers, and conversely, the conditions under which the hand can prevent all possible motions of the object. The dual view is that one needs to know the set of wrenches that the hand can apply to the object and under what conditions any wrench in $\mathbb{R}^6$ can be applied through the contacts. This knowledge will be gained by studying the various subspaces associated with $\boldsymbol{G}$ and $\boldsymbol{J}$ [28.13].

The spaces, shown in Fig. 28.3, are the column spaces and null spaces of $\boldsymbol{G}$, $\boldsymbol{G}^\top$, $\boldsymbol{J}$, and $\boldsymbol{J}^\top$. Column space (also known as range) and null space will be denoted by $\mathcal{R}(\cdot)$ and $\mathcal{N}(\cdot)$, respectively. The arrows show the propagation of the various velocity and load quantities through the grasping system. For example, in the left part of Fig. 28.3 it is shown how any vector $\dot{\boldsymbol{q}} \in \mathbb{R}^{n_q}$ can be decomposed into a sum of two orthogonal vectors in

$\mathcal{R}(\boldsymbol{J}^\top)$ and in $\mathcal{N}(\boldsymbol{J})$ and how $\dot{\boldsymbol{q}}$ is mapped to $\mathcal{R}(\boldsymbol{J})$ by multiplication by $\boldsymbol{J}$.
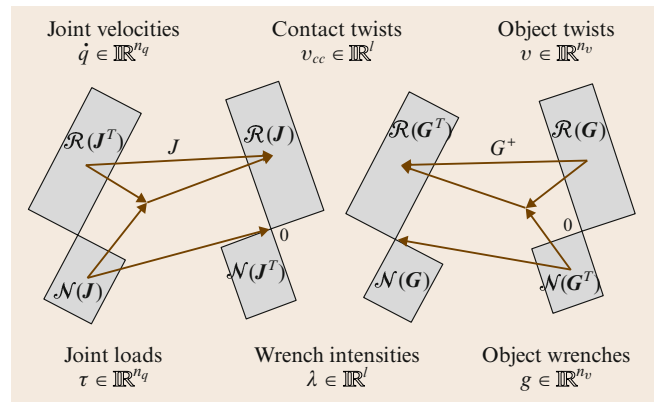
Fig. 28.3 Linear maps relating the twists and wrenches of a grasping system

Part D | Manipulation and Interfaces

Table 28.5 Basic grasp classes

Condition	Class	Many to one
$\mathcal{N}(J) \neq \mathbf{0}$	Redundant	$\dot{q} \rightarrow v_{cc}$ $\tau \rightarrow \lambda$
$\mathcal{N}(G^\top) \neq \mathbf{0}$	Indeterminate	$v \rightarrow v_{cc}$ $g \rightarrow \lambda$
$\mathcal{N}(G) \neq \mathbf{0}$	Graspable	$\lambda \rightarrow g$ $v_{cc} \rightarrow v$
$\mathcal{N}(J^\top) \neq \mathbf{0}$	Defective	$\lambda \rightarrow \tau$ $v_{cc} \rightarrow \dot{q}$

It is important to recall two facts from linear algebra. First, a matrix A maps vectors from $\mathcal{R}(A^\top)$ to $\mathcal{R}(A)$ in a one-to-one and onto fashion, that is, the map A is a bijection. The generalized inverse A^+ of A is a bijection that maps vectors in the opposite direction [28.14]. Also, A maps vectors in $\mathcal{N}(A)$ to zero. Finally, there is no nontrivial vector that A can map into $\mathcal{N}(A^\top)$. This implies that, if $\mathcal{N}(G^\top)$ is nontrivial, then the hand will not be able to control all degrees of freedom of the object's motion. This is certainly true for quasistatic grasping, but when dynamics are important, they may cause the object to move along the directions in $\mathcal{N}(G^\top)$.

28.3.1 Grasp Classifications

The four null spaces motivate a basic classification of grasping systems defined in Table 28.5. Assuming solutions to (28.21) exist, the following force and velocity equations provide insight into the physical meaning of the various null spaces:

$$\dot{q} = J^+ v_{cc} + N(J)\alpha , \qquad (28.24)$$

$$v = (G^\top)^+ v_{cc} + N(G^\top)\beta , \qquad (28.25)$$

$$\lambda = -G^+ g + N(G)\gamma , \qquad (28.26)$$

$$\lambda = (J^\top)^+ \tau + N(J^\top)\eta . \qquad (28.27)$$

In these equations, A^+ denotes the generalized inverse, henceforth pseudoinverse, of a matrix A, $N(A)$ denotes a matrix whose columns form a basis for $\mathcal{N}(A)$, and α, β, γ, and η are arbitrary vectors that parameterize the solution sets. If not otherwise specified, the context will make clear whether the generalized inverse is left or right.

If the null spaces represented in the equations are nontrivial, then one immediately sees the first many-to-one mapping in the Table 28.5. To see the other many-to-one mappings, and in particular the defective class, consider (28.24). It can be rewritten with v_{cc} de-

composed into components v_{rs} and v_{lns} in $\mathcal{R}(J)$ and $\mathcal{N}(J^\top)$, respectively, as follows:

$$\dot{q} = J^+(v_{rs} + v_{lns}) + N(J)\alpha . \qquad (28.28)$$

Recall that every vector in $\mathcal{N}(A^\top)$ is orthogonal to every row of A^+. Therefore $J^+ v_{lns} = \mathbf{0}$. If α and v_{rs} are fixed in (28.28), then $\dot{q}$ is unique. Thus it is clear that, if $\mathcal{N}(J^\top)$ is nontrivial, then a subspace of twists of the hand at the contacts will map to a single joint velocity vector. Applying the same approach to the other three equations (28.25–28.27) yields the other many-to-one mappings listed in Table 28.5.

Equations (28.21) and (28.24–28.27), motivate the following definitions.

Definition 28.1 Redundant
A grasping system is said to be *redundant* if $\mathcal{N}(J)$ is nontrivial.

Joint velocities $\dot{q}$ in $\mathcal{N}(J)$ are referred to as *internal hand velocities*, since they correspond to finger motions, but do not generate motion of the hand in the constrained directions at the contact points. If the quasistatic model applies, it can be shown that these motions are not influenced by the motion of the object and vice versa.

Definition 28.2 Indeterminate
A grasping system is said to be *indeterminate* if $\mathcal{N}(G^\top)$ is nontrivial.

Object twists v in $\mathcal{N}(G^\top)$ are called *internal object twists*, since they correspond to motions of the object, but do not cause motion of the object in the constrained directions at the contacts. If the static model applies, it can be shown that these twists cannot be controlled by finger motions.

Definition 28.3 Graspable
A grasping system is said to be *graspable* if $\mathcal{N}(G)$ is nontrivial.

Wrench intensities λ in $\mathcal{N}(G)$ are referred to as *internal object forces*. These wrenches are *internal* because they do not contribute to the acceleration of the object, i. e., $G\lambda = \mathbf{0}$. Instead, these wrench intensities affect the tightness of the grasp. Thus, internal wrench intensities play a fundamental role in maintaining grasps that rely on friction (Sect. 28.5.2).

Definition 28.4 Defective

A grasping system is said to be *defective* if $\mathcal{N}(\boldsymbol{J}^{\top})$ is nontrivial.

Wrench intensities $\boldsymbol{\lambda}$ in $\mathcal{N}(\boldsymbol{J}^{\top})$ are called *internal hand forces*. These forces do not influence the hand joint dynamics given in (28.20). If the static model is considered, it can be easily shown that wrench intensities belonging to $\mathcal{N}(\boldsymbol{J}^{\top})$ cannot be generated by joint actions, but can be resisted by the structure of the hand.

See Example 1, Part 4; Example 2, Part 2; and Example 3, Part 3.

28.3.2 Limitations of Rigid–Body Assumption

The rigid-body dynamics equation (28.20) can be rewritten with Lagrange multipliers associated with the contact constraints as:

$$\boldsymbol{M}_{\mathrm{dyn}} \begin{pmatrix} \ddot{\boldsymbol{q}} \\ \dot{\boldsymbol{v}} \\ \boldsymbol{\lambda} \end{pmatrix} = \begin{pmatrix} \boldsymbol{\tau} - \boldsymbol{b}_{\mathrm{hnd}} \\ \boldsymbol{v} - \boldsymbol{b}_{\mathrm{obj}} \\ \boldsymbol{b}_{\mathrm{c}} \end{pmatrix} , \qquad (28.29)$$

where $\boldsymbol{b}_{\mathrm{c}} = [\partial(\boldsymbol{J}\dot{\boldsymbol{q}})/\partial\boldsymbol{q}]\dot{\boldsymbol{q}} - [\partial(\boldsymbol{G}\boldsymbol{v})/\partial\boldsymbol{u}]\dot{\boldsymbol{u}}$ and

$$\boldsymbol{M}_{\mathrm{dyn}} = \begin{pmatrix} \boldsymbol{M}_{\mathrm{hnd}} & \boldsymbol{0} & \boldsymbol{J}^{\top} \\ \boldsymbol{0} & \boldsymbol{M}_{\mathrm{obj}} & -\boldsymbol{G} \\ \boldsymbol{J} & -\boldsymbol{G}^{\top} & \boldsymbol{0} \end{pmatrix} .$$

In order for this equation to determine the motion of the system completely, it is necessary that the matrix $\boldsymbol{M}_{\mathrm{dyn}}$ be invertible. This case is considered in detail in [28.15], where the dynamics of multifinger manipulation is studied under the hypothesis that the hand Jacobian is full row rank, $\mathcal{N}(\boldsymbol{J}^{\top}) = \boldsymbol{0}$. For all manipulation systems with noninvertible $\boldsymbol{M}_{\mathrm{dyn}}$, rigid-body dynamics fails to determine the motion and the wrench intensity vector. By observing that:

$$\mathcal{N}(\boldsymbol{M}_{\mathrm{dyn}})$$
$$= \{(\ddot{\boldsymbol{q}}, \dot{\boldsymbol{v}}\boldsymbol{\lambda})^{\top} | \ddot{\boldsymbol{q}} = \boldsymbol{0}, \dot{\boldsymbol{v}} = \boldsymbol{0}, \boldsymbol{\lambda} \in \mathcal{N}(\boldsymbol{J}^{\top}) \cap \mathcal{N}(\boldsymbol{G})\} ,$$

the same arguments apply under the quasistatic conditions defined by (28.21) and (28.23). When $\mathcal{N}(\boldsymbol{J}^{\top}) \cap \mathcal{N}(\boldsymbol{G}) \neq \boldsymbol{0}$, the rigid-body approach fails to solve the first equation in (28.21), thus leaving $\boldsymbol{\lambda}$ indeterminate.

Definition 28.5 Hyperstatic

A grasping system is said to be *hyperstatic* if $\mathcal{N}(\boldsymbol{J}^{\top}) \cap \mathcal{N}(\boldsymbol{G})$ is nontrivial.

In such systems there are internal forces (Definition 28.3) belonging to $\mathcal{N}(\boldsymbol{J}^{\top})$ that are not controllable as discussed for defective grasps. Rigid-body dynamics is not satisfactory for hyperstatic grasps since the rigid-body assumption leads to undetermined contact wrenches [28.16].

See Example 3, Part 3.

28.3.3 Desirable Properties

For a general-purpose grasping system, there are three main desirable properties: control of the object twist $\boldsymbol{v}$, control of object wrench $\boldsymbol{g}$, and control of the internal forces. Control of these quantities implies that the hand can deliver the desired $\boldsymbol{v}$ and $\boldsymbol{g}$ with specified grip pressure by the appropriate choice of joint velocities and actions. The conditions on $\boldsymbol{J}$ and $\boldsymbol{G}$ equivalent to these properties are given in Table 28.6.

We derive the associated conditions in two steps. First, we ignore the structure and configuration of the hand (captured in $\boldsymbol{J}$) by assuming that the contact point on the finger can be commanded to move in any direction transmitted by the chosen contact model. An important perspective here is that $\boldsymbol{v}_{cc}$ is seen as the independent input variable and $\boldsymbol{v}$ is seen as the output. The dual interpretation is that the actuators can generate any contact force and moment in the constrained directions. Similarly, $\boldsymbol{\lambda}$ is seen as the input and $\boldsymbol{g}$ is seen as the output. The preliminary property of interest under this assumption is whether or not the arrangement and types of contacts on the object (captured in $\boldsymbol{G}$) are such that a sufficiently dexterous hand could control its fingers so as to impart any twist $\boldsymbol{v} \in \mathbb{R}^6$ to the object and, similarly, to apply any wrench $\boldsymbol{g} \in \mathbb{R}^6$ to the object.

All Object Twists Possible

Given a set of contact locations and types, by solving (28.19) for $\boldsymbol{v}$ or observing the map $\boldsymbol{G}$ on the right side of Fig. 28.3, one sees that the achievable object twists are those in $\mathcal{R}(\boldsymbol{G})$. Those in $\mathcal{N}(\boldsymbol{G}^{\top})$ could not be achieved by any hand using the given grasp. Therefore, to achieve any object twist, we must have: $\mathcal{N}(\boldsymbol{G}^{\top}) = \boldsymbol{0}$, or equiva-

Table 28.6 Desirable properties of a grasp

Task requirement	Required conditions
All wrenches possible, $\boldsymbol{g}$ All twists possible, $\boldsymbol{v}$	$\mathrm{rank}(\boldsymbol{G}) = n_v$
Control all wrenches, $\boldsymbol{g}$ Control all twists, $\boldsymbol{v}$	$\begin{cases} \mathrm{rank}(\boldsymbol{G}) = n_v \\ \mathrm{rank}(\boldsymbol{GJ}) = n_v \end{cases}$
Control all internal forces	$\mathcal{N}(\boldsymbol{G}) \cap \mathcal{N}(\boldsymbol{J}^{\top}) = \boldsymbol{0}$

Fig. 28.4 The Salisbury hand

lently, rank$(G) = n_v$. Any grasp with three non-collinear hard contacts or two distinct soft contacts satisfies this condition.

All Object Wrenches Possible

This case is the dual of the previous case, so we expect the same condition. From (28.21), one immediately obtains the condition $\mathcal{N}(G^\top) = \mathbf{0}$, so again we have rank$(G) = n_v$.

To obtain the conditions needed to control the various quantities of interest, the structure of the hand cannot be ignored. Recall that the only achievable contact twists on the hand are in $\mathcal{R}(J)$, which is not necessarily equal to $\mathbb{R}^\ell$.

Control All Object Twists

By solving (28.17) for v, one sees that, in order to cause any object twist v by choice of joint velocities $\dot{q}$, we must have $\mathcal{R}(GJ) = \mathcal{R}(G)$ and $\mathcal{N}(G^\top) = 0$. These conditions are equivalent to rank$(GJ) = $ rank$(G) = n_v$.

Control All Object Wrenches

This property is dual to the previous one. Analysis of (28.21) yields the same conditions: rank$(GJ) = $ rank$(G) = n_v$.

Control All Internal Forces

Equation (28.20) shows that wrench intensities with no effect on object motion are only those in $\mathcal{N}(G)$. In general, not all the internal forces may be actively controlled by joint actions. In [28.12, 17] it has been shown that all internal forces in $\mathcal{N}(G)$ are controllable if and only if $\mathcal{N}(G) \cap \mathcal{N}(J^\top) = \mathbf{0}$.

See Example 1, Part 5 and Example 2, Part 3.

Design Considerations of the Salisbury Hand

The Salisbury hand in Fig. 28.4 was designed to have the smallest number of joints that would meet all the task requirements in Table 28.6. Assuming HF contacts, three non-collinear contacts is the minimum number such that rank$(G) = n_v = 6$. In this case, G has six rows and nine columns and the dimension of $\mathcal{N}(G)$ is three [28.1, 4]. The ability to control all internal forces and apply an arbitrary wrench to the object requires that $\mathcal{N}(G) \cap \mathcal{N}(J^\top) = \mathbf{0}$, so the minimum dimension of the column space of J is nine. To achieve this, the hand must have at least nine joints, which Salisbury implemented as three fingers, each with three revolute joints.

The intended way to execute a dexterous manipulation task with the Salisbury hand is to grasp the object at three non-collinear points with the fingertips, forming a grasp triangle. To secure the grasp, the internal forces are controlled so that the contact points are maintained without sliding. Dexterous manipulation can be thought of as moving the fingertips to control the positions of the vertices of the grasp triangle.

28.4 Restraint Analysis

The most fundamental requirements in grasping and dexterous manipulation are the abilities to hold an object in equilibrium and control the position and orientation of the grasped object relative to the palm of the hand. The two most useful characterizations of grasp restraint are *force closure* and *form closure*. These names were in use over 125 years ago in the field of machine design to distinguish between joints that required an external force to maintain contact, and those that did not [28.18]. For example, some water wheels had a cylindrical axle that

was laid in a horizontal semicylindrical groove split on either side of the wheel. During operation, the weight of the wheel acted to *close* the groove–axle contacts, hence the term *force closure*. By contrast, if the grooves were replaced by cylindrical holes just long enough to accept the axle, then the contacts would be closed by the geometry (even if the direction of the gravitational force were reversed), hence the term *form closure*.

When applied to grasping, form and force closure have the following interpretations. Assume that a hand

Fig. 28.5 The palm, fingers, wrist, and watch band combine to create a very secure form closure grasp of a TV remote controller

grasping an object has its joint angles locked and its palm fixed in space; then the grasp has *form closure*, or the object is *form closed*, if it is impossible to move the object, even infinitesimally. Under the same conditions, the grasp has *force closure*, or the object is *force closed*, if for any noncontact wrench experienced by the object, contact wrench intensities exist that satisfy (28.20) and are consistent with the constraints imposed by the friction models applicable at the contact points. Notice that all form closure grasps are also force closure grasps. When under form closure, the object cannot move at

Fig. 28.6 This grasp has a force closure grasp appropriate for dexterous manipulation (Image of Shadow Dextrous Hand © Shadow Robot Company 2008)

Fig. 28.7 In the grasp depicted, contact with the ridges on the gasoline cap creates partial form closure in the direction of cap rotation (when screwing it in) and also in the directions of translation perpendicular to the axis of rotation. To achieve complete control over the cap, the grasp achieves force closure over the other three degrees of freedom

all, regardless of the noncontact wrench. Therefore, the hand maintains the object in equilibrium for any external wrench, which is the force closure requirement.

Roughly speaking, form closure occurs when the palm and fingers wrap around the object forming a cage with no *wiggle room* such as the grasp shown in Fig. 28.5. This kind of grasp is also called a *power grasp* [28.19] or an *enveloping grasp* [28.20]. However, force closure is possible with fewer contacts, as shown in Fig. 28.6, but in this case force closure requires the ability to control internal forces. It is also possible for a grasp to have partial form closure, indicating that only a subset of the possible degrees of freedom are restrained by form closure [28.21]. An example of such a grasp is shown in Fig. 28.7. In this grasp, fingertip placement between the ridges around the periphery of the gasoline cap provide form closure against relative rotation about the axis of the helix of the threads and also against translation perpendicular to that axis, but the other three degrees of freedom are restrained through force closure. Strictly speaking, given a grasp of a real object by a human hand, it is impossible to prevent relative motion of the object with respect to the palm due to the compliance of the hand and object. Preventing all motion is possible only if the contacting bodies are rigid, as is assumed in most mathematical models employed in grasp analysis.

28.4.1 Form Closure

To make the notion of form closure precise, introduce a gap function denoted by $\psi_i(\boldsymbol{u}, \boldsymbol{q})$ at each of the n_c contact points between the object and the hand. The gap function is zero at each contact, becomes positive if contact breaks, and negative if penetration occurs. The

gap function can be thought of as the distance between the contact points. In general, this function is dependent on the shapes of the contacting bodies. Let $\bar{u}$ and $\bar{q}$ represent the configurations of the object and hand for a given grasp; then:

$$\psi_i(\bar{u}, \bar{q}) = 0 \quad \forall\, i = 1, \ldots, n_c . \tag{28.30}$$

The form closure condition can now be stated in terms of a differential change du of $\bar{u}$:

Definition 28.6

A grasp $(\bar{u}, \bar{q})$ has *form closure* if and only if the following implication holds:

$$\psi(\bar{u} + du, \bar{q}) \geq 0 \Rightarrow du = 0 , \tag{28.31}$$

where ψ is the n_c-dimensional vector of gap functions with i-th component equal to $\psi_i(u, q)$. By definition, inequalities between vectors imply that the inequality is applied between corresponding components of the vectors.

Expanding the gap function vector in a Taylor series about $\bar{u}$ yields infinitesimal form closure tests of various orders. Let $^\beta\psi(u, q)$, $\beta = 1, 2, 3, \ldots$ denote the Taylor series approximation truncated after the terms of order β in du. From (28.30), it follows that the first-order approximation is:

$$^1\psi(\bar{u} + du, \bar{q}) = \left.\frac{\partial \psi(u, q)}{\partial u}\right|_{(\bar{u}, \bar{q})} du ,$$

where $\partial\psi(u, q)/\partial u|_{(\bar{u}, \bar{q})}$ denotes the partial derivative of ψ with respect to u evaluated at $(\bar{u}, \bar{q})$. Replacing ψ with its approximation of order β in (28.31) implies three relevant cases of order β:

1. if there exists du such that $^\beta\psi(\bar{u} + du, \bar{q})$ has at least one strictly positive component, then the grasp does not have form closure of order β;
2. if for every nonzero du, $^\beta\psi(\bar{u} + du, \bar{q})$ has at least one strictly negative component, then the grasp has form closure of order β;
3. if neither case 1 nor case 2 applies for all $^\alpha\psi(\bar{u} + du, \bar{q}) \,\forall\, \alpha \leq \beta$, then higher-order analysis is required to determine the existence of form closure.

Figure 28.8 illustrates form closure concepts using several planar grasps of gray objects by fingers shown as dark disks. The concepts are identical for grasps of three-dimensional objects, but are more clearly illustrated in a plane. The grasp on the left has first-order form closure. Note that first-order form closure only involves the first derivatives of the distance functions. This implies that the only relevant geometry in first-order form closure are the locations of the contacts and the directions of the contact normals. The grasp in the center has form closure of higher order, with the specific order depending on the degrees of the curves defining the surfaces of the object and fingers in the neighborhoods of the contacts [28.22]. Second-order form closure analysis depends on the curvatures of the two contacting bodies in addition to the geometric information used to analyze first-order form closure. The grasp on the right does not have form closure of any order, because the object can translate horizontally and rotate about its center.

First-Order Form Closure

First-order form closure exists if and only if the following implication holds:

$$\left.\frac{\partial \psi(u, q)}{\partial u}\right|_{(\bar{u}, \bar{q})} du \geq 0 \Rightarrow du = 0 .$$

The first-order form closure condition can be written in terms of the object twist v:

$$G_n^\top v \geq 0 \Rightarrow v = 0 , \tag{28.32}$$

where $G_n^\top = \partial\psi/\partial u\, V \in \mathbb{R}^{n_c \times 6}$. Because the gap functions only quantify distances, the product $G_n^\top v$ is the vector of normal components of the instantaneous velocities of the object at the contact points (which must be nonnegative to prevent interpenetration). This in turn implies that the grasp matrix is the one that would result from the assumption that all contacts are of the type PwoF.

An equivalent condition in terms of the contact wrench intensity vector $\lambda_n \in \mathbb{R}^{n_c}$ can be stated as follows. A grasp has first-order form closure if and only

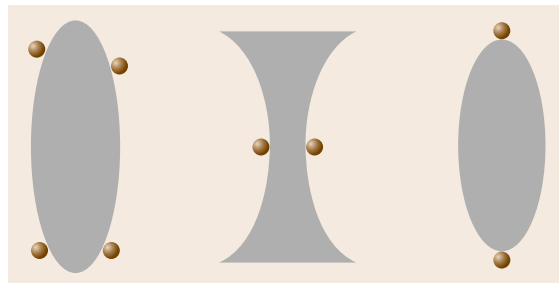**Fig. 28.8** Three planar grasps: two with form closure of different orders and one without form closure

if:

$$\left.\begin{array}{l} G_n \lambda_n = -g \\ \lambda_n \geq 0 \end{array}\right\} \forall g \in \mathbb{R}^6 . \tag{28.33}$$

The physical interpretation of this condition is that equilibrium can be maintained under the assumption that the contacts are frictionless. Note that the components of λ_n are the magnitudes of the normal components of the contact forces. The subscript $(.)_n$ is used to emphasize that λ_n contains no other force or moment components.

Since g must be in the range of G_n for equilibrium to be satisfied, and since g is an arbitrary element of $\mathbb{R}^6$, then in order for condition (28.33) to be satisfied, the rank of G_n must be six. Assuming $\text{rank}(G_n) = 6$, another equivalent mathematical statement of first-order form closure is: there exists λ_n such that the following two conditions hold [28.23]:

$$G_n \lambda_n = 0 , \\ \lambda_n > 0 . \tag{28.34}$$

This means that there exists a set of strictly compressive normal contact forces in the null space of G_n. In other words, one can squeeze the object as tightly as desired while maintaining equilibrium. A second interpretation of this condition is that the nonnegative span of the columns of G_n must equal $\mathbb{R}^6$. As will be seen, this interpretation will provide a conceptual link called *frictional form closure* that lies between form closure and force closure.

The duality of conditions (28.32) and (28.33) can be seen clearly by examining the set of wrenches that can be applied by frictionless contacts and the corresponding set of possible object twists. For this discussion, it is useful to give definitions of cones and their duals.

Definition 28.7
A *cone* $\mathcal{C}$ is a set of vectors ς such that, for every ς in $\mathcal{C}$, every nonnegative scalar multiple of ς is also in $\mathcal{C}$.

Equivalently, a cone is a set of vectors closed under addition and nonnegative scalar multiplication.

Table 28.7 Minimum number of contacts n_c required to form close an object with n_v degrees of freedom

n_v	n_c
3 (planar grasp)	4
6 (spatial grasp)	7
n_v (general)	$n_v + 1$

Definition 28.8
Given a cone $\mathcal{C}$ with elements ς, the *dual cone* $\mathcal{C}^*$ with elements ς^* is the set of vectors such that the dot product of ς^* with each vector in $\mathcal{C}$ is nonnegative. Mathematically:

$$\mathcal{C}^* = \{\varsigma^* | \varsigma^\top \varsigma^* \geq 0, \forall \varsigma \in \mathcal{C}\} . \tag{28.35}$$

See Example 4.

First-Order Form Closure Requirements
Several useful necessary conditions for form closure are known. In 1897 *Somov* proved that at least seven contacts are necessary to form close a rigid object with six degrees of freedom [28.24]. *Lakshminarayana* generalized this to prove that $n_v + 1$ contacts are necessary to form close an object with n_v degrees of freedom [28.21] (based on *Goldman* and *Tucker* 1956 [28.25]), see Table 28.7. This led to the definition of partial form closure that was mentioned above in the discussion of the hand grasping the gasoline cap. *Markenscoff* and *Papadimitriou* determined a tight upper bound, showing that, for all objects whose surfaces are not surfaces of revolution, at most $n_v + 1$ contacts are necessary [28.26]. Form closure is impossible to achieve for surfaces of revolution.

To emphasize the fact that $n_v + 1$ contacts are necessary and *not* sufficient, consider grasping a cube with seven or more points of contact. If all contacts are on one face, then clearly the cube is not form closed.

First-Order Form Closure Tests
Because form closure grasps are very secure, it is desirable to design or synthesize such grasps. To do this, one needs a way to test candidate grasps for form closure, and rank them so that the *best* grasp can be chosen. One reasonable measure of form closure can be derived from the geometric interpretation of the condition (28.34). The null space constraint and the positivity of λ_n represent the addition of the columns of G_n scaled by the components of λ_n. Any choice of λ_n closing this loop is in $\mathcal{N}(G_n)$. For a given loop, if the magnitude of the smallest component of λ_n is positive, then the grasp has form closure, otherwise it does not. Let us denote this smallest component by d. Since such a loop, and hence d, can be scaled arbitrarily, λ_n should be bounded for computational expediency.

After verifying that G_n has full row rank, a quantitative form closure test based on the above observations can be formulated as a linear program (LP) in the

unknowns d and $\boldsymbol{\lambda}_n$ as follows:

$$\textit{LP1:} \quad \text{maximize}: \quad d \qquad (28.36)$$
$$\text{subject to}: \quad \boldsymbol{G}_n \boldsymbol{\lambda}_n = \mathbf{0} \qquad (28.37)$$
$$\boldsymbol{I}\boldsymbol{\lambda}_n - \boldsymbol{1}d \geq \mathbf{0} \qquad (28.38)$$
$$d \geq 0 \qquad (28.39)$$
$$\mathbf{1}^\top \boldsymbol{\lambda}_n \leq n_c, \qquad (28.40)$$

where $\boldsymbol{I} \in \mathbb{R}^{n_c \times n_c}$ is the identity matrix and $\boldsymbol{1} \in \mathbb{R}^n_c$ is a vector with all components equal to 1. The last inequality is designed to prevent this LP from becoming unbounded. A typical LP solution algorithm determines infeasibility or unboundedness of the constraints in the, so-called, phase I of the algorithm, and considers the result before attempting to calculate an optimal value [28.27]. If *LP1* is infeasible, or if the optimal value d^* is zero, then the grasp is not form closed.

The quantitative form closure test (28.36–28.40) has $n_c + 8$ constraints and $n_c + 1$ unknowns. For a typical grasp with $n_c < 10$, this is a small linear program that can be solved very quickly using the simplex method. However, one should note that the metric d^* is dependent on the choice of units used when forming $\boldsymbol{G}_n$. It would be advisable to nondimensionalize the components of the wrenches to avoid dependence of the optimal d on ones choice of units. This could be done by dividing the first three rows of $\boldsymbol{G}$ by a characteristic force and the last three rows by a characteristic moment.

However, if one desires a binary test, *LP1* can be converted into one by dropping the last constraint (28.40) and applying only phase I of the simplex algorithm.

In summary, form closure testing is a two-step process:

Form Closure Test
1. Compute rank($\boldsymbol{G}_n$).
   a) If rank($\boldsymbol{G}_n$) $\neq n_v$, then form closure does not exist. Stop.
   b) If rank($\boldsymbol{G}_n$) $= n_v$, continue.
2. Solve *LP1*.
   a) If $d^* = 0$, then form closure does not exist.
   b) If $d^* > 0$, then form closure exists and d^* is a crude measure of how far the grasp is from losing form closure.

Variations of the Test
If the rank test fails, then the grasp could have partial form closure over as many as rank($\boldsymbol{G}_n$) degrees of freedom. If one desires to test this, then *LP1* must be solved using a new $\boldsymbol{G}_n$ formed by retaining only the rows cor-
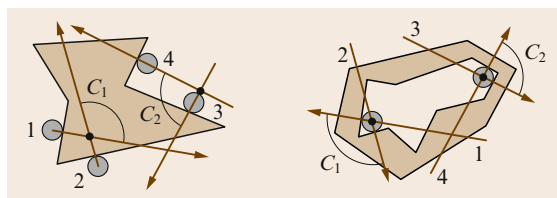

Fig. 28.9 Planar grasps with first-order form closure

responding to the degrees of freedom for which partial form closure is to be tested. If $d^* > 0$, then partial form closure exists. A second variation is to constrain d to be greater than some large negative value. If this is done, then $d^* < 0$ is a crude measure of how far a grasp is from achieving form closure.

See Example 5.

Planar Simplifications
In the planar case, *Nguyen* [28.28] developed a graphical qualitative test for form closure. Figure 28.9 shows two form closure grasps with four contacts. To test form closure one partitions the normals into two groups of two. Let $\mathcal{C}_1$ be the nonnegative span of two normals in one pair and $\mathcal{C}_2$ be the nonnegative span of the other pair. A grasp has form closure if and only if $\mathcal{C}_1$ and $\mathcal{C}_2$ or $-\mathcal{C}_1$ and $-\mathcal{C}_2$ *see each other* for any pairings. Two cones *see each other* if the open line segment defined by the vertices of the cones lies in the interior of both cones. In the presence of more than four contacts, if any set of four contacts satisfies this condition, then the grasp has form closure. Notice that this graphical test can be difficult to execute for grasps with more than four contacts. Also, it does not extend to grasps of three-dimensional (3-D) objects and does not provide a closure measure.

28.4.2 Force Closure

A grasp has force closure, or is force closed, if the grasp can be maintained in the face of any object wrench. Force closure is similar to form closure, but relaxed to allow friction forces to help balance the object wrench. A benefit of including friction in the analysis is the reduction in the number of contact points needed for closure. A three-dimensional object with six degrees of freedom requires seven contacts for form closure, but for force closure, only two contacts are needed if they are modeled as soft fingers, and only three (non-collinear) contacts are needed if they are modeled as hard fingers.

Force closure relies on the ability of the hand to squeeze arbitrarily tightly in order to compensate for large applied wrenches that can only be resisted by

Table 28.8 Norms for the three main contact models

Model	$\|\lambda_i\|_w$
PwoF	0
HF	$\frac{1}{\mu_i}\sqrt{f_{it}^2 + f_{io}^2}$
SF	$\frac{1}{\mu_i}\sqrt{f_{it}^2 + f_{io}^2} + \frac{1}{av_i}|m_{in}|$

friction. Figure 28.14 shows a grasped polygon (see Example 2). Consider applying a wrench to the object that is a pure force acting upward along the y-axis of the inertial frame. It seems intuitive that, if there is enough friction, the hand will be able to squeeze the object with friction forces preventing the object's upward escape. Also, as the applied force increases in magnitude, the magnitude of the squeezing force will have to increase accordingly.

Since force closure is dependent on the friction models, common models will be introduced before giving formal definitions of force closure.

Friction Models

Recall the components of force and moment transmitted through contact i under the various contact models given earlier (Table 28.4). At contact point i, the friction law imposes constraints on the components of the contact force and moment. Specifically, the frictional components of λ_i are constrained to lie inside a limit surface, denoted by $\mathcal{L}_i$, that scales linearly with the product $\mu_i f_{in}$, where μ_i is the coefficient of friction at contact i. In the case of Coulomb friction, the limit surface is a circle of radius $\mu_i f_{in}$. The Coulomb friction cone $\mathcal{F}_i$ is a subset of $\mathbb{R}^3$:

$$\mathcal{F}_i = \left\{ (f_{in}, f_{it}, f_{io}) | \sqrt{f_{it}^2 + f_{io}^2} \le \mu_i f_{in} \right\} . \quad (28.41)$$

More generally, the friction laws of interest have limit surfaces defined in the space of friction components, $\mathbb{R}^{\ell_i - 1}$, and friction cones $\mathcal{F}_i$ defined in the space of λ_i, $\mathbb{R}^{\ell_i}$. They can be written as

$$\mathcal{F}_i = \left\{ \lambda_i \in \mathbb{R}^{\ell_i} \mid \|\lambda_i\|_w \le f_{in} \right\} , \quad (28.42)$$

where $\|\lambda_i\|_w$ denotes a weighted quadratic norm of the friction components at contact i. The limit surface is defined by $\|\lambda_i\|_w = f_{in}$.

Table 28.8 defines useful weighted quadratic norms for the three contact models: PwoF, HF, and SF. The parameter μ_i is the friction coefficient for the tangential forces, v_i is the torsional friction coefficient, and a is the characteristic length of the object that is used to ensure consistent units in the terms of the norm of the SF model.

Remark. There are several noteworthy points to be made about the friction cones. First, all of them implicitly or explicitly constrain the normal component of the contact force to be nonnegative. The cone for SF contacts has a cylindrical limit surface with circular cross section in the (f_{it}, f_{io})-plane and rectangular cross section in the (f_{it}, m_{in})-plane. With this model, the amount of torsional friction that can be transmitted is independent of the lateral friction load. An improved model that couples the torsional friction limit with the tangential limit was studied by *Howe* and *Cutkosky* [28.29].

A Force Closure Definition

One common definition of force closure can be stated simply by modifying condition (28.33) to allow each contact force to lie in its friction cone rather than along the contact normal. Because this definition does not consider the hand's ability to control contact forces, this definition will be referred to as *frictional form closure*. A grasp will be said to have frictional form closure if and only if the following conditions are satisfied:

$$\left. \begin{array}{l} G\lambda = -g \\ \lambda \in \mathcal{F} \end{array} \right\} \forall g \in \mathbb{R}^{n_v} ,$$

where $\mathcal{F}$ is the composite friction cone defined as: $\mathcal{F} = \mathcal{F}_1 \times \cdots \times \mathcal{F}_{n_c} = \{\lambda \in \mathbb{R}^m | \lambda_i \in \mathcal{F}_i; i = 1, \ldots, n_c\}$, and each $\mathcal{F}_i$ is defined by (28.42) and one of the models listed in Table 28.8.

Letting $\text{Int}(\mathcal{F})$ denote the interior of the composite friction cone, *Murray* et al. give the following equivalent definition [28.15]:

Definition 28.9

(Proposition 5.2, Murray et al.) A grasp has *frictional form closure* if and only if the following conditions are satisfied:

1. $\text{rank}(G) = n_v$
2. $\exists \lambda$ such that $G\lambda = 0$ and $\lambda \in \text{Int}(\mathcal{F})$.

These conditions define what Murray et al. call *force closure*. The force closure definition adopted here is stricter than frictional form closure; it additionally requires that the hand be able to control the internal object forces.

Definition 28.10

A grasp has *force closure* if and only if $\text{rank}(G) = n_v$, $\mathcal{N}(G) \cap \mathcal{N}(J^\top) = 0$, and there exists λ such that $G\lambda = 0$ and $\lambda \in \text{Int}(\mathcal{F})$.

The full row rank condition on the matrix G is the same condition required for form closure, although G is different from G_n used to determine form closure. If the rank test passes, then one must still find λ satisfying the remaining three conditions. Of these, the null space intersection test can be performed easily by linear programming techniques, but the friction cone constraint is quadratic, and thus forces one to use nonlinear programming techniques. While exact nonlinear tests have been developed [28.30], only approximate tests will be presented here.

Approximate Force Closure Tests

Any of the friction cones discussed can be approximated as the nonnegative span of a finite number n_g of generators s_{ij} of the friction cone. Given this, one can represent the set of applicable contact wrenches at contact i as follows:

$$G_i \lambda_i = S_i \sigma_i, \quad \sigma_i \geq 0,$$

where $S_i = (s_{i1} \cdots s_{in_g})$ and σ_i is a vector of nonnegative generator weights. If contact i is frictionless, then $n_g = 1$ and $S_i = [\hat{n}_i^\top \quad (c_i - p) \times \hat{n}_i)^\top]^\top$.

If contact i is of type HF, we represent the friction cone by the nonnegative sum of uniformly spaced contact force generators (Fig. 28.10) whose nonnegative span approximates the Coulomb cone with an inscribed regular polyhedral cone. This leads to the following definition of S_i:

$$S_i = \begin{pmatrix} \cdots & 1 & \cdots \\ \cdots & \mu_i \cos(2k\pi/n_g) & \cdots \\ \cdots & \mu_i \sin(2k\pi/n_g) & \cdots \end{pmatrix}, \quad (28.43)$$
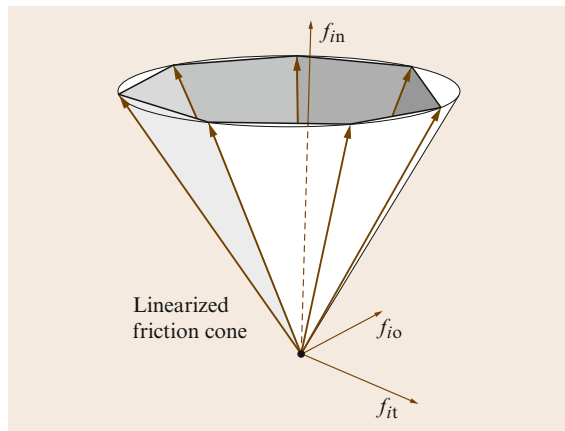

Fig. 28.10 Quadratic cone approximated as a polyhedral cone with seven generators

where the index k varies from 1 to n_g. If one prefers to approximate the quadratic friction cone by a circumscribing polyhedral cone, one simply replaces μ_i in the above definition with $\mu_i / \cos(\pi n_g)$.

The adjustment needed for the SF model is quite simple. Since the torsional friction in this model is decoupled from the tangential friction, its generators are given by $[1 \quad 0 \quad 0 \quad \pm b\upsilon_i]^\top$. Thus S_i for the SF model is:

$$S_i = \begin{pmatrix} \cdots & 1 & \cdots & 1 & 1 \\ \cdots & \mu_i \cos(2k\pi/n_g) & \cdots & 0 & 0 \\ \cdots & \mu_i \sin(2k\pi/n_g) & \cdots & 0 & 0 \\ \cdots & 0 & \cdots & b\upsilon_i & -b\upsilon_i \end{pmatrix}, \quad (28.44)$$

where b is the characteristic length used to unify units. The set of total contact wrenches that may be applied by the hand without violating the contact friction law at any contact can be written as:

$$G\lambda = S\sigma, \quad \sigma \geq 0,$$

where $S = (S_1, \cdots, S_{n_g})$ and $\sigma = (\sigma_1^\top \quad \cdots \quad \sigma_{n_g}^\top)^\top$.

It is convenient to reformulate the friction constraints in a dual form:

$$F_i \lambda_i \geq 0. \quad (28.45)$$

In this form, each row of F_i is normal to a face formed by two adjacent generators of the approximate cone. For an HF contact, row i of F_i can be computed as the cross product of s_i and s_{i+1}. In the case of an SF contact, the generators are of dimension four, so simple cross products will not suffice. However, general methods exist to perform the conversion from the generator form to the face normal form [28.25].

The face normal constraints for all contacts can be combined into the following compact form:

$$F\lambda \geq 0, \quad (28.46)$$

where $F = \text{Blockdiag}(F_1, \ldots, F_{n_c})$.

Let $e_i \in \mathbb{R}^{\ell_i}$ be the first row of H_i. Further let $e = (e_1, \ldots, e_{n_c}) \in \mathbb{R}^\ell$ and let $E = \text{Blockdiag}(e_1, \ldots, e_{n_c}) \in \mathbb{R}^{\ell \times n_c}$. The following linear program is a quantitative test for frictional form closure. The optimal objective function value d^* is a measure of the distance the contact forces are from the boundaries of their friction cones, and hence a crude measure of how far a grasp is from

losing frictional form closure.

LP2:   maximize : d

subject to: $G\lambda = 0$

$F\lambda - \mathbf{1}d \geq 0$

$d \geq 0$

$e\lambda \leq n_c$.

The last inequality in *LP2* is simply the sum of the magnitudes of the normal components of the contact forces. After solving *LP2*, if $d^* = 0$ frictional form closure does not exist, but if $d^* > 0$, then it does.

If the grasp has frictional form closure, the last step to determine the existence of force closure is to verify the condition $\mathcal{N}(G) \cap \mathcal{N}(J^\top) = \mathbf{0}$. If it holds, then the grasp has force closure. This condition is easy to verify with another linear program *LP3*.

LP3:   maximize : d

subject to: $G\lambda = 0$

$J^\top \lambda = 0$

$E\lambda - \mathbf{1}d \geq 0$

$d \geq 0$

$e\lambda \leq n_c$.

In summary, force closure testing is a three-step process:

Approximate Force Closure Test

1. Compute rank(G).
   a) If rank(G) $\neq n_v$, then force closure does not exist. Stop.

b) If rank(G) $= n_v$, continue.
2. Solve *LP2: Test frictional form closure.*
   a) If $d^* = 0$, then frictional form closure does not exist. Stop.
   b) If $d^* > 0$, then frictional form closure exists and d^* is a crude measure of how far the grasp is from losing frictional form closure.
3. Solve *LP3. Test control of internal force.*
   a) If $d^* > 0$, then force closure does not exist.
   b) If $d^* = 0$, then force closure exists.

See Example 1, Part 6.

Planar Simplifications

In planar grasping systems, the approximate method described above is exact. This is because the SF models are meaningless, since rotations about the contact normal would cause motions out of the plane. With regard to the HF model, for planar problems, the quadratic friction cone becomes linear, with its cone represented exactly as:

$$F_i = \frac{1}{\sqrt{1 + \mu_i^2}} \begin{pmatrix} \mu_i & 1 \\ \mu_i & -1 \end{pmatrix} . \tag{28.47}$$

Nguyen's graphical form closure test can be applied to planar grasps with two frictional contacts [28.28]. The only change is that the four contact normals are replaced by the four generators of the two friction cones. However, the test can only determine frictional form closure, since it does not incorporate the additional information needed to determine force closure.

28.5 Examples

28.5.1 Example 1: Grasped Sphere

Part 1: $\tilde{G}$ and $\tilde{J}$

Figure 28.11 shows a planar projection of a three-dimensional sphere of radius r grasped by two fingers, which make two contacts at angles θ_1 and θ_2. The frames $\{C\}_1$ and $\{C\}_2$ are oriented so that their $\hat{o}$-directions point out of the plane of the figure (as indicated by the small bold circle). The axes of the frames $\{N\}$ and $\{B\}$ were chosen to be axis-aligned with coincident origins located at the center of the sphere. The z-axes are pointing out of the page. Observe that, since the two joint axes of the left finger are perpendicular to the (x, y)-plane, it operates in that plane for all time. The other finger has three revolute joints. Because its first and second axes, $\hat{z}_3$ and $\hat{z}_4$, currently lie in the plane, rotation about $\hat{z}_3$ will cause $\hat{z}_4$ to attain an out-of-plane component and would cause the finger tip at contact 2 to leave the plane.

In the current configuration, the rotation matrix for the i-th contact frame is defined as

$$R_i = \begin{pmatrix} -\cos(\theta_i) & \sin(\theta_i) & 0 \\ -\sin(\theta_i) & -\cos(\theta_i) & 0 \\ 0 & 0 & 1 \end{pmatrix} . \tag{28.48}$$

The vector from the origin of $\{N\}$ to the i-th contact point is given by

$$c_i - p = r \begin{pmatrix} \cos(\theta_i) & \sin(\theta_i) & 0 \end{pmatrix}^\top . \tag{28.49}$$

Fig. 28.11 A sphere grasped by a two-fingered hand with five revolute joints

Substituting into (28.3) and (28.6) yields the complete grasp matrix for contact i:

$$
\tilde{G}_i = \left(
\begin{array}{ccc|ccc}
-c_i & s_i & 0 & & & \\
-s_i & -c_i & 0 & & \mathbf{0} & \\
0 & 0 & 1 & & & \\
\hline
0 & 0 & rs_i & -c_i & s_i & 0 \\
0 & 0 & -rc_i & -s_i & -c_i & 0 \\
0 & -r & 0 & 0 & 0 & 1
\end{array}
\right), \qquad (28.50)
$$

where $\mathbf{0} \in \mathbb{R}^{3\times3}$ is the zero matrix and c_i and s_i are abbreviations for $\cos(\theta_i)$ and $\sin(\theta_i)$, respectively. The complete grasp matrix is defined as: $\tilde{G} = (\tilde{G}_1\ \tilde{G}_2) \in \mathbb{R}^{6\times12}$.

The accuracy of this matrix can be verified by inspection; for example, the first column is the unit wrench of the unit contact normal, the first three components are the direction cosines of $\hat{n}_i$, and the last three are $(c_i - p) \times \hat{n}_i$. Since $\hat{n}_i$ is collinear with $(c_i - p)$, the cross products (the last three components of the column) are zero. The last three components of the second column represent the moment of $\hat{t}_i$ about the x-, y-, and z-axes of $\{N\}$. Since $\hat{t}_i$ lies in the (x, y)-plane, the moments with the x- and y-axes are zero. Clearly $\hat{t}_i$ produces a moment of $-r$ about the z-axis.

Construction of the complete hand Jacobian $\tilde{J}_i$ for contact i requires knowledge of the joint axis directions and the origins of the frames fixed to the links of

Fig. 28.12 Relevant data for the hand Jacobian

each finger. Figure 28.12 shows the hand in the same configuration as in Fig. 28.11, but with some additional data needed to construct the hand Jacobian. Assume that the origins of the joint frames lie in the plane of the figure.

In the current configuration, the quantities of interest for contact 1, expressed in $\{C\}_1$ are:

$$
c_1 - \zeta_1 = \begin{pmatrix} l_2 & l_1 & 0 \end{pmatrix}^\top, \qquad (28.51)
$$

$$
c_1 - \zeta_2 = \begin{pmatrix} l_7 & l_3 & 0 \end{pmatrix}^\top, \qquad (28.52)
$$

$$
\hat{z}_1 = \hat{z}_2 = \begin{pmatrix} 0 & 0 & 1 \end{pmatrix}^\top. \qquad (28.53)
$$

The quantities of interest for contact 2, in $\{C\}_2$ are:

$$
c_2 - \zeta_3 = c_2 - \zeta_4 = \begin{pmatrix} l_4 & -l_5 & 0 \end{pmatrix}^\top, \qquad (28.54)
$$

$$
c_2 - \zeta_5 = \begin{pmatrix} l_6 & 0 & 0 \end{pmatrix}^\top, \qquad (28.55)
$$

$$
\hat{z}_3 = \begin{pmatrix} 0 & -1 & 0 \end{pmatrix}^\top, \qquad (28.56)
$$

$$
\hat{z}_4(q_3) = \frac{\sqrt{2}}{2} \begin{pmatrix} -1 & -1 & 0 \end{pmatrix}^\top, \qquad (28.57)
$$

$$
\hat{z}_5(q_3, q_4) = \begin{pmatrix} 0 & 0 & 1 \end{pmatrix}^\top. \qquad (28.58)
$$

Generally all of the components of the $c - \zeta$ and $\hat{z}$ vectors (including the components that are zero in the current configuration) are functions of q and u. The dependencies of the $\hat{z}$ vectors are shown explicitly.

Substituting into (28.14), (28.11), and (28.8) yields the complete hand Jacobian $\tilde{J} \in \mathbb{R}^{12 \times 5}$:

$$\tilde{J} = \left(\begin{array}{ccccc} -l_1 & -l_3 & & & \\ l_2 & l_7 & & & \\ 0 & 0 & & & \\ 0 & 0 & & \mathbf{0} & \\ 0 & 0 & & & \\ 1 & 1 & & & \\ \hline & & 0 & 0 & 0 \\ & & 0 & 0 & l_6 \\ & & l_4 & \frac{\sqrt{2}}{2}(l_4+l_5) & 0 \\ \mathbf{0} & & 0 & -\frac{\sqrt{2}}{2} & 0 \\ & & -1 & -\frac{\sqrt{2}}{2} & 0 \\ & & 0 & 0 & 1 \end{array} \right).$$

The horizontal dividing line partitions $\tilde{J}$ into $\tilde{J}_1$ (on top) and $\tilde{J}_2$ (on the bottom). The columns correspond to joints 1–5. The block diagonal structure is a result of the fact that finger i directly affects only contact i.

Example 1, Part 2: G and J

Assume that the contacts in Fig. 28.11 are both of type SF. Then the selection matrix H is given by

$$H = \left(\begin{array}{cccccc|c} 1 & 0 & 0 & 0 & 0 & 0 & \\ 0 & 1 & 0 & 0 & 0 & 0 & \mathbf{0} \\ 0 & 0 & 1 & 0 & 0 & 0 & \\ 0 & 0 & 0 & 1 & 0 & 0 & \\ \hline & & & & & & 1\ 0\ 0\ 0\ 0\ 0 \\ & & \mathbf{0} & & & & 0\ 1\ 0\ 0\ 0\ 0 \\ & & & & & & 0\ 0\ 1\ 0\ 0\ 0 \\ & & & & & & 0\ 0\ 0\ 1\ 0\ 0 \end{array} \right),$$

thus the matrices $G^\top \in \mathbb{R}^{8 \times 6}$ and $J \in \mathbb{R}^{8 \times 5}$ are constructed by removing rows 5, 6, 11, and 12 from $\tilde{G}^\top$ and $\tilde{J}$:

$$G^\top = \left(\begin{array}{cccccc} -c_1 & -s_1 & 0 & 0 & 0 & 0 \\ s_1 & -c_1 & 0 & 0 & 0 & -r \\ 0 & 0 & 1 & rs_1 & -rc_1 & 0 \\ 0 & 0 & 0 & -c_1 & -s_1 & 0 \\ \hline -c_2 & -s_2 & 0 & 0 & 0 & 0 \\ s_2 & -c_2 & 0 & 0 & 0 & -r \\ 0 & 0 & 1 & rs_2 & -rc_2 & 0 \\ 0 & 0 & 0 & -c_2 & -s_2 & 0 \end{array} \right), \quad (28.59)$$

$$J = \left(\begin{array}{cc|ccc} -l_1 & -l_3 & & & \\ l_2 & l_7 & & \mathbf{0} & \\ 0 & 0 & & & \\ 0 & 0 & & & \\ \hline & & 0 & 0 & 0 \\ & & 0 & 0 & l_6 \\ \mathbf{0} & & d & \frac{\sqrt{2}}{2}(l_4+l_5) & 0 \\ & & 0 & -\frac{\sqrt{2}}{2} & 0 \end{array} \right). \quad (28.60)$$

Notice that changing the contact models is easily accomplished by removing more rows. Changing contact 1 to HF would eliminate the fourth rows from $G^\top$ and J, while changing it to PwoF would eliminate the second, third, and fourth rows of $G^\top$ and J. Changing the model at contact 2 would remove either just the eighth row or the sixth, seventh, and eighth rows.

Example 1, Part 3: Reduction to the Planar Case

The grasp shown in Fig. 28.11 can be reduced to a planar problem by following the explicit formulas given above, but it can also be done by understanding the physical interpretations of the various rows and columns of the matrices. Proceed by eliminating velocities and forces that are out of the plane. This can be done by removing the z-axes from $\{N\}$ and $\{B\}$, and the $\hat{o}$-directions at the contacts. Further, joints 3 and 4 must be locked. The resulting $G^\top$ and J are constructed eliminating certain rows and columns. $G^\top$ is formed by removing rows 3, 4, 7, and 8 and columns 3, 4, and 5. J is formed by removing rows 3, 4, 7, and 8 and columns 3 and 4,

Table 28.9 Dimensions of the main subspaces and classifications of the grasp studied in Example 1

Models	Dimension	Class
HF,HF	dim $\mathcal{N}(J) = 1$	Redundant
	dim $\mathcal{N}(G^\top) = 1$	Indeterminate
	dim $\mathcal{N}(G) = 1$	Graspable
	dim $\mathcal{N}(J^\top) = 2$	Defective
SF,HF	dim $\mathcal{N}(J) = 1$	Redundant
	dim $\mathcal{N}(G) = 1$	Graspable
	dim $\mathcal{N}(J^\top) = 3$	Defective
HF,SF	dim $\mathcal{N}(G) = 1$	Graspable
	dim $\mathcal{N}(J^\top) = 2$	Defective
SF,SF	dim $\mathcal{N}(G) = 2$	Graspable
	dim $\mathcal{N}(J^\top) = 3$	Defective

yielding:

$$G^\top = \begin{pmatrix} -c_1 & -s_1 & 0 \\ s_1 & -c_1 & -r \\ -c_2 & -s_2 & 0 \\ s_2 & -c_2 & -r \end{pmatrix}, \quad (28.61)$$

$$J = \begin{pmatrix} -l_1 & -l_3 & 0 \\ l_2 & l_7 & 0 \\ 0 & 0 & 0 \\ 0 & 0 & l_6 \end{pmatrix}. \quad (28.62)$$

Example 1, Part 4: Grasp Classes

The first column of Table 28.9 reports the dimensions of the main subspaces of J and G for the sphere grasping example with different contact models. Only nontrivial null spaces are listed.

In the case of two HF contact models, all four null spaces are nontrivial, so the system satisfies the conditions for all four grasp classes. The system is graspable because there is an internal force along the line segment connecting the two contact points. Indeterminacy is manifested in the fact that the hand cannot resist a moment acting about that line. Redundancy is seen to exist since joint 3 can be used to move contact 2 out of the plane of the figure, but joint 4 can be rotated in the opposite direction to cancel this motion. Finally, the grasp is defective, because the contact forces and the instantaneous velocities along the $\hat{o}_1$ and $\hat{n}_2$ directions of contact 1 and 2, respectively, cannot be controlled through the joint torques and velocities. These interpretations are borne out in the null space basis matrices below, computed using $r = 1$, $\cos(\theta_1) = -0.8 = -\cos(\theta_2)$, $\sin(\theta_1) = \cos(\theta_2) = -0.6$, and $l_7 = 0$:

$$N(J) \approx \begin{pmatrix} 0 \\ 0 \\ -0.73 \\ 0.69 \\ 0 \end{pmatrix}, \quad N(G^\top) \approx \begin{pmatrix} 0 \\ 0 \\ 0.51 \\ 0.86 \\ 0 \\ 0 \end{pmatrix}, \quad (28.63)$$

$$N(G) \approx \begin{pmatrix} 0.57 \\ -0.42 \\ 0 \\ 0.57 \\ 0.42 \\ 0 \end{pmatrix}, \quad N(J^\top) = \begin{pmatrix} 0 & 0 \\ 0 & 0 \\ 0 & -1 \\ 1 & 0 \\ 0 & 0 \\ 0 & 0 \end{pmatrix}. \quad (28.64)$$

Notice that changing either contact to SF makes it possible for the hand to resist external moments applied about the line containing the contacts, so the grasp loses indeterminacy, but retains graspability (with squeezing still possible along the line of the contacts). However, if contact 2 is the SF contact, the grasp loses its redundancy. While the second contact point can still be moved out of the plane by joint 3 and back in by joint 4, this canceled translation of the contact point yields a net rotation about $\hat{n}_2$ (this also implies that the hand can control the moment applied to the object along the line containing the contacts). Changing to SF at contact 2 does *not* affect the hand's inability to move contact 1 and contact 2 in the $\hat{o}_1$ and $\hat{n}_2$ directions, so the defectivity property is retained.

Example 1, Part 5: Desirable Properties

Assuming contact model types of SF and HF at contacts 1 and 2, respectively, G is full row rank and so $\mathcal{N}(G^\top) = 0$ (Table 28.9). Therefore, as long as the the hand is sufficiently dexterous, it can apply any wrench in $\mathbb{R}^6$ to the object. Also, if the joints are locked, object motion will be prevented. Assuming the same problem values used in the previous part of this problem, the matrix $G^\top$ is:

$$G^\top = \begin{pmatrix} -c_1 & -s_1 & 0 & 0 & 0 & 0 \\ s_1 & -c_1 & 0 & 0 & 0 & -r \\ 0 & 0 & 1 & rs_1 & -rc_1 & 0 \\ 0 & 0 & 0 & -c_1 & -s_1 & 0 \\ -c_2 & -s_2 & 0 & 0 & 0 & 0 \\ s_2 & -c_2 & 0 & 0 & 0 & -r \\ 0 & 0 & 1 & rs_2 & -rc_2 & 0 \end{pmatrix}. \quad (28.65)$$

Bases for the three nontrivial null spaces are:

$$N(J^\top) = \begin{pmatrix} 0 & 0 & 0 \\ 0 & 0 & 0 \\ 0 & 0 & -1 \\ 1 & 0 & 0 \\ 0 & -1 & 0 \\ 0 & 0 & 0 \\ 0 & 0 & 0 \end{pmatrix}, \quad (28.66)$$

$$N(J) \approx \begin{pmatrix} 0 \\ 0 \\ -0.73 \\ 0.69 \\ 0 \end{pmatrix},$$

$$N(G) \approx \begin{pmatrix} 0.57 \\ -0.42 \\ 0 \\ 0 \\ 0.57 \\ 0.42 \\ 0 \end{pmatrix}. \tag{28.67}$$

Since $\mathcal{R}(J)$ is four dimensional and $\mathcal{N}(G)$ is one dimensional, the maximum dimension of $\mathcal{R}(J) + \mathcal{N}(G)$ cannot be more than five, and therefore, the hand cannot control all possible object velocities, for example, the contact velocity $v_{cc} = (0\,0\,0\,0.8\,0\,0\,0)^\top$ is in $\mathcal{N}(J^\top)$, and so cannot be controlled by the fingers. It is also equal to 0.6 times the third column of $G^\top$ plus the fourth column of $G^\top$ and therefore is in $\mathcal{R}(G^\top)$. Since the mapping between $\mathcal{R}(G)$ and $\mathcal{R}(G^\top)$ is one to one and onto, this uncontrollable contact velocity corresponds to a unique uncontrollable object velocity, $v = (0\,0\,0.6\,1\,0\,0)$. In other words, the hand cannot cause the center of the sphere to translate in the z-direction, while also rotating about the x-axis (and not other axes simultaneously).

On the question of controlling all internal object forces, the answer is *yes*, since $\mathcal{N}(J^\top) \cap \mathcal{N}(G) = 0$. This conclusion is clear from the fact that $\mathcal{N}(G)$ has nonzero values in the first, second, and sixth positions, while all columns of $\mathcal{N}(J^\top)$ have zeros in those positions.
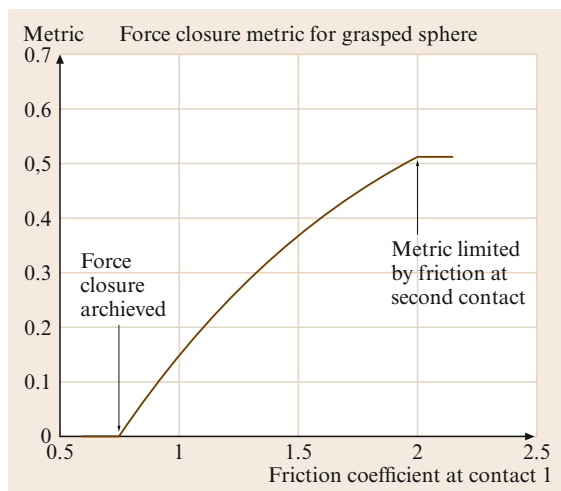

Fig. 28.13 Plot of the force closure metric versus the friction coefficient on contact 1

Example 1, Part 6: Force Closure

Again assume that contacts 1 and 2 on the grasped sphere were modeled as SF and HF contacts, respectively. Under this assumption, G is full row rank, and the internal force corresponds to equal and opposite contact forces. For frictional form closure to exist, the internal force must lie within the friction cones. Choosing r and the sines and cosines of θ_1 and θ_2 as in example 1, part 4, frictional form closure can be shown to exist if both friction coefficients are greater than 0.75. For this grasp, since $\mathcal{N}(J^\top) \cap \mathcal{N}(G) = 0$, frictional form closure is equivalent to force closure.

The plot in Fig. 28.13 was generated by fixing $\mu_2 = 2.0$ and varying μ_1. Notice that, for $\mu_1 < 0.75$, force closure does not exist. The metric increases smoothly until μ_1 becomes equal to μ_2. At this point, increasing μ_1 further does not improve force closure, since contact 2 becomes the limiting factor. To increase the metric further, both friction coefficients must be increased.

28.5.2 Example 2: Grasped Polygon in the Plane

Part 1: G and J

Figure 28.14 shows a planar hand grasping a polygon. Finger 1 (on the right) contains two joints numbered 1 and 2. Finger 2 contains joints 3–7, which are numbered in increasing order moving from the palm distally. The inertial frame has been chosen to lie inside the object, with its x-axis passing through contacts 1 and 2, and collinear with the normal vector of contact 2.
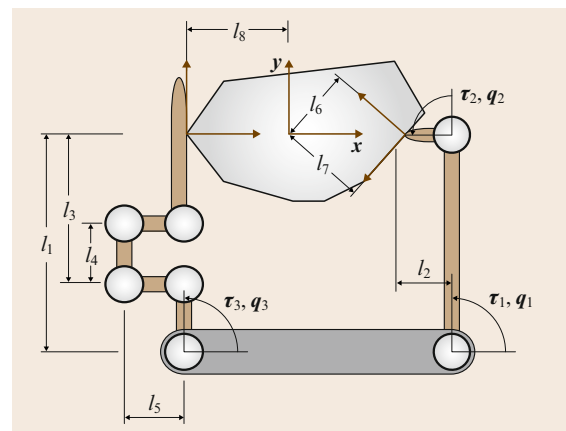

Fig. 28.14 Planar hand with two fingers and seven joints grasping a polygonal object

The rotation matrices are given by

$$R_1 = \begin{pmatrix} -0.8 & -0.6 \\ 0.6 & -0.8 \end{pmatrix}, \quad R_2 = \begin{pmatrix} 1 & 0 \\ 0 & 1 \end{pmatrix}. \qquad (28.68)$$

Assuming HF contacts, G is given as

$$G = \begin{pmatrix} -0.8 & -0.6 & 1 & 0 \\ 0.6 & -0.8 & 0 & 1 \\ l_6 & -l_7 & 0 & -l_8 \end{pmatrix}. \qquad (28.69)$$

Notice that the first two columns of G correspond to the normal and tangential unit vectors at contact 1. The third and fourth columns correspond to contact 2.

Assuming HF contacts and that all joints are active (i. e., not locked), J is

$$J^\top = \begin{pmatrix} 0.8l_1 & 0.6l_1 & & \\ -0.6l_2 & 0.8l_2 & & \mathbf{0} \\ \hline & & -l_1 & 0 \\ & & -l_3 & 0 \\ & \mathbf{0} & -l_3 & l_5 \\ & & -l_3 + l_4 & l_5 \\ & & -l_3 + l_4 & 0 \end{pmatrix}. \qquad (28.70)$$

The first two columns of $J^\top$ are the torques required to produce a unit force in the $\hat{\boldsymbol{n}}_1$ and $\hat{\boldsymbol{t}}_1$ directions at contact 1. The horizontal line through the matrix partitions the contributions for the first finger (the upper part) and second finger. Notice that both $J^\top$ and G are full column rank.

Example 2, Part 2: Grasp Classes

This example clearly illustrates the physical qualities of the various grasp classes without introducing features that can cloud the descriptions.

We now discuss the details of the four grasp classes using the previous planar example. During these discussions it is useful to choose nondimensional values for the parameters in the grasping system. Assume l_4 is the unit length. The other lengths as fractions of l_4 are:

$$l_1 = 2.7, \quad l_2 = 1.0, \quad l_3 = 1.7, \qquad (28.71)$$

$$l_4 = 1.0, \quad l_5 = 1.0, \quad l_6 = 1.0, \qquad (28.72)$$

$$l_7 = 1.3, \quad l_8 = 1.5. \qquad (28.73)$$

Redundant

Redundancy exists if $\mathcal{N}(J)$ is nontrivial. Assuming that both contacts are hard contacts and that all the joints

are active, $\text{rank}(J) = 4$, so $\mathcal{N}(J)$ is three dimensional. A basis for $\mathcal{N}(J)$ was obtained as

$$N(J) \approx \begin{pmatrix} 0 & 0 & 0 \\ 0 & 0 & 0 \\ -0.50 & -0.24 & -0.18 \\ 0.53 & 0.67 & -0.10 \\ 0.48 & -0.49 & -0.02 \\ -0.48 & 0.49 & 0.02 \\ -0.02 & 0.01 & 0.98 \end{pmatrix}. \qquad (28.74)$$

Since the first two rows are zero, $\mathcal{N}(J)$ does not include motions of the first finger (on the right of the palm). To understand this, assume that the object is fixed in the plane. Then the first finger cannot maintain sticking contact at contact 1 unless its joints are also fixed.

The three nonzero columns corresponding to finger 2 show that there are three basis motions of its joints that allow the finger contact to stick to the object contact. For example, the first column shows that, if joint 3 moves roughly as much as joints 4, 5, and 6, but in the opposite direction as joints 4 and 5 and in the same direction as joint 6, while joint 7 is more or less fixed, then contact 2 will be maintained.

Notice that finger 2 contains a parallelogram. Because of this geometry, one can see that the vector $(0\,0\,0 -1\,1 -1\,1)^\top$ is an element of $\mathcal{N}(J)$. The velocity interpretation of this vector is that the link of the finger connected to the palm, and the link touching the object remain fixed in space, while the parallelogram moves as a simple four-bar mechanism. Similarly, joint actions in $\mathcal{N}(J)$ do not affect the contact forces, but cause internal hand velocities. Also, notice that, since $\mathcal{N}(J^\top) = \mathbf{0}$, the entire space of possible generalized velocities and forces at the contacts can be generated by the joints.

Indeterminate

As noted above, with HF contact models, the system is graspable. However, replacing the HF models with PwoF models removes the tangent force components in the $\hat{\boldsymbol{t}}_1$ and $\hat{\boldsymbol{t}}_2$ directions. This effectively removes columns 2 and 4 from G, which guarantees that the system will be indeterminate. The reduced matrix is denoted by $G_{(1,3)}$. In this case $\mathcal{N}(G_{(1,3)}^\top)$ is

$$N(G_{(1,3)}^\top) \approx \begin{pmatrix} 0 \\ -0.86 \\ 0.51 \end{pmatrix}. \qquad (28.75)$$

Physically, this basis vector corresponds to moving the object such that the point coincident with the origin of $\{N\}$ moves directly downward, while the object rotates counterclockwise. Also, if the analogous force and moment were applied to the object, the frictionless contacts could not maintain equilibrium.

Graspable

With two HF contact models in force, $\text{rank}(G) = 3$, so $\mathcal{N}(G)$ is one dimensional and the system is graspable. The null space basis vector of the grasp matrix is:

$$N(G) \approx \begin{pmatrix} 0.57 \\ 0.42 \\ 0.71 \\ 0 \end{pmatrix}. \tag{28.76}$$

The physical interpretation of this basis vector is two opposing forces acting through the two contact points. Recall that, because the contact model is kinematic, there is no consideration of contact friction. However, given the direction of the contact normal relative to the line of the internal force, one can see that if the coefficient of friction is not greater than 0.75, squeezing tightly will cause sliding at contact 1, thus violating the kinematic contact model.

Defective

In a defective grasp, $\mathcal{N}(J^\top) \neq 0$. Given that the original J is full row rank, the grasp is *not* defective. However, it can be made defective by locking a number of joints and/or changing the hand's configuration so that J is no longer full rank. For example, locking joints 4, 5, 6, and 7 makes finger 2 a single-link finger with only joint 3 active. In this new grasping system, $J^\top_{(1,2,3)}$ is simply the first three rows of the original $J^\top$ given in (28.70), where the subscript is the list of indices of active joints. The null space basis vector is:

$$N(J^\top_{(1,2,3)}) = \begin{pmatrix} 0 \\ 0 \\ 0 \\ 1 \end{pmatrix}. \tag{28.77}$$

This grasp is defective, since there is a subspace of contact velocities and forces that cannot be controlled by joint generalized velocities and forces. Since only the last component of $N(J^\top_{(1,2,3)})$ is nonzero, it
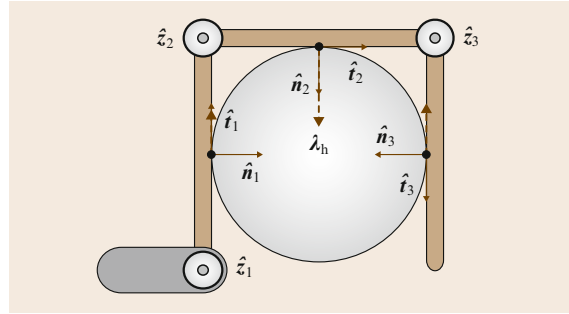

Fig. 28.15 A sphere grasped by a finger with three revolute joints. The force direction λ_h (*dashed line*) is a force that belongs to both $\mathcal{N}(G)$ and $\mathcal{N}(J^\top)$ and causes hyperstaticity

would be impossible for the hand to give the contact point 2 on the object a velocity in the $\hat{t}_2$-direction while maintaining the contact. This is also clear from the arrangement of joint 3, contact 2, and the direction of the contact normal. The dual interpretation is that forces in $\mathcal{N}(J^\top)$ are resisted by the structure and the corresponding joint loads is zero, or equivalently that those forces are not controllable by the hand. Notice that if the model of contact 2 were changed to point without friction, then $N(J^\top_{(1,2,3)}) = 0$ and the system would no longer be defective.

28.5.3 Example 3: Hyperstatic Grasps

Part 1: $\tilde{G}$ and $\tilde{J}$

Figure 28.15 shows a planar projection of a three-dimensional sphere of radius l grasped by one finger only, with three revolute joints, through three contacts. The frames $\{C\}_1$, $\{C\}_2$, and $\{C\}_3$ are oriented so that their $\hat{o}$-directions point out of the plane of the figure (as indicated by the small bold circle). The axes of the frames $\{N\}$ and $\{B\}$ were chosen to be axis-aligned with coincident origins located at the center of the sphere. The z-axes are pointing out of the page. Observe that since the three joint axes of the finger are perpendicular to the (x, y)-plane, the grasp operates in that plane for all time.

Assume that the width of all the links of the robotic hand is zero. Rotation matrices R_i and vectors $c_i - p$ for $i = 1, \dots, 3$, can be computed as in (28.48) and (28.49) considering that $\theta_1 = \pi$, for contact 1, $\theta_2 = \pi/2$ and $\theta_3 = 0$, for contacts 2 and 3, respectively. Finally, the complete grasp matrix is $\tilde{G}^\top = \begin{pmatrix} \tilde{G}_1 & \tilde{G}_2 & \tilde{G}_2 \end{pmatrix}^\top \in \mathbb{R}^{18 \times 6}$

where $\tilde{G}_i$ is as defined in (28.50):

$$\tilde{G}^\top = \left(\begin{array}{cccccc}
1 & 0 & 0 & 0 & 0 & 0 \\
0 & 1 & 0 & 0 & 0 & -l \\
0 & 0 & 1 & 0 & l & 0 \\
0 & 0 & 0 & 1 & 0 & 0 \\
0 & 0 & 0 & 0 & 1 & 0 \\
0 & 0 & 0 & 0 & 0 & 1 \\
\hline
0 & -1 & 0 & 0 & 0 & 0 \\
1 & 0 & 0 & 0 & 0 & -l \\
0 & 0 & 1 & l & 0 & 0 \\
0 & 0 & 0 & 0 & -1 & 0 \\
0 & 0 & 0 & 1 & 0 & 0 \\
0 & 0 & 0 & 0 & 0 & 1 \\
\hline
-1 & 0 & 0 & 0 & 0 & 0 \\
0 & -1 & 0 & 0 & 0 & -l \\
0 & 0 & 1 & 0 & -l & 0 \\
0 & 0 & 0 & -1 & 0 & 0 \\
0 & 0 & 0 & 0 & -1 & 0 \\
0 & 0 & 0 & 0 & 0 & 1
\end{array}\right) .$$

Construction of the complete hand Jacobian $\tilde{J}_i$ for contact i requires knowledge of the joint axis directions and the origins of the frames fixed to the links of each finger. Assume that the origins of the DH frames lie in the plane of the figure. In the current configuration, the quantities of interest for contact 1, expressed directly in $\{N\}$, are

$$c_1 - \zeta_1 = \begin{pmatrix} 0 & l & 0 \end{pmatrix}^\top ,$$
$$\hat{z}_1 = \begin{pmatrix} 0 & 0 & 1 \end{pmatrix}^\top .$$

The quantities of interest for contact 2, in $\{N\}$, are

$$c_2 - \zeta_1 = \begin{pmatrix} l & 2l & 0 \end{pmatrix}^\top ,$$
$$c_2 - \zeta_2 = \begin{pmatrix} l & 0 & 0 \end{pmatrix}^\top ,$$
$$\hat{z}_1 = \begin{pmatrix} 0 & 0 & 1 \end{pmatrix}^\top ,$$
$$\hat{z}_2 = \begin{pmatrix} 0 & 0 & 1 \end{pmatrix}^\top .$$

The quantities of interest for contact 3, in $\{N\}$, are

$$c_3 - \zeta_1 = \begin{pmatrix} 2l & l & 0 \end{pmatrix}^\top ,$$
$$c_3 - \zeta_2 = \begin{pmatrix} 2l & -l & 0 \end{pmatrix}^\top ,$$

$$c_3 - \zeta_3 = \begin{pmatrix} 0 & -l & 0 \end{pmatrix}^\top ,$$
$$\hat{z}_1 = \begin{pmatrix} 0 & 0 & 1 \end{pmatrix}^\top ,$$
$$\hat{z}_2 = \begin{pmatrix} 0 & 0 & 1 \end{pmatrix}^\top ,$$
$$\hat{z}_3 = \begin{pmatrix} 0 & 0 & 1 \end{pmatrix}^\top .$$

The complete hand Jacobian $\tilde{J} \in \mathbb{R}^{18 \times 3}$ (contact velocities are expressed in $\{C\}_i$) is:

$$\tilde{J} = \left(\begin{array}{ccc}
-l & 0 & 0 \\
0 & 0 & 0 \\
0 & 0 & 0 \\
0 & 0 & 0 \\
0 & 0 & 0 \\
1 & 0 & 0 \\
\hline
-l & -l & 0 \\
-2l & 0 & 0 \\
0 & 0 & 0 \\
0 & 0 & 0 \\
0 & 0 & 0 \\
1 & 1 & 0 \\
\hline
l & -l & -l \\
-2l & -2l & 0 \\
0 & 0 & 0 \\
0 & 0 & 0 \\
0 & 0 & 0 \\
1 & 1 & 1
\end{array}\right) .$$

The horizontal dividing line partitions $\tilde{J}$ into $\tilde{J}_1$ (on top), $\tilde{J}_2$, and $\tilde{J}_3$ (on the bottom). The columns correspond to joints 1–3.

Example 3, Part 2: G and J

Assume that the three contacts in Fig. 28.15 are of type HF. Then the selection matrix H is given by

$$H = \begin{pmatrix} I & 0 & 0 & 0 & 0 & 0 \\ 0 & 0 & I & 0 & 0 & 0 \\ 0 & 0 & 0 & 0 & I & 0 \end{pmatrix} , \tag{28.78}$$

where I and 0 are in $\mathbb{R}^{3 \times 3}$, thus the matrices $G^\top \in \mathbb{R}^{9 \times 6}$ and $J \in \mathbb{R}^{9 \times 3}$ are obtained by removing rows related to

rotations from $\tilde{\boldsymbol{G}}^\top$ and $\tilde{\boldsymbol{J}}$:

$$\boldsymbol{G}^\top = \begin{pmatrix} 1 & 0 & 0 & 0 & 0 & 0 \\ 0 & 1 & 0 & 0 & 0 & -l \\ 0 & 0 & 1 & 0 & l & 0 \\ \hline 0 & -1 & 0 & 0 & 0 & 0 \\ 1 & 0 & 0 & 0 & 0 & -l \\ 0 & 0 & 1 & l & 0 & 0 \\ \hline -1 & 0 & 0 & 0 & 0 & 0 \\ 0 & -1 & 0 & 0 & 0 & -l \\ 0 & 0 & 1 & 0 & -l & 0 \end{pmatrix} ,$$

$$\boldsymbol{J} = \begin{pmatrix} l & 0 & 0 \\ 0 & 0 & 0 \\ 0 & 0 & 0 \\ \hline l & l & 0 \\ 2l & 0 & 0 \\ 0 & 0 & 0 \\ \hline l & l & l \\ 2l & 2l & 0 \\ 0 & 0 & 0 \end{pmatrix} .$$

Example 3, Part 3: Grasp Classes

The first column of Table 28.10 reports the dimensions of the main subspaces of $\boldsymbol{J}^\top$ and $\boldsymbol{G}$ for the sphere grasping example with three hard-finger contacts. Only nontrivial null spaces are listed.

The system is defective because there are generalized contact forces belonging to the subspace that are resisted by the structure, which correspond to zero joint actions:

$$N(\boldsymbol{J}^\top) = \begin{pmatrix} 0 & 0 & 0 & 0 & -2 & 0 \\ 0 & 0 & 0 & 1 & 0 & 0 \\ 0 & 0 & 1 & 0 & 0 & 0 \\ \hline 0 & 0 & 0 & 0 & 0 & -2 \\ 0 & 0 & 0 & 0 & 1 & 0 \\ 0 & 1 & 0 & 0 & 0 & 0 \\ \hline 0 & 0 & 0 & 0 & 0 & 0 \\ 0 & 0 & 0 & 0 & 0 & 1 \\ 1 & 0 & 0 & 0 & 0 & 0 \end{pmatrix} .$$

The first three columns represent generalized forces acting at the three contact points in a direction perpendicular to the plane of the Fig. 28.15. The fourth column corresponds to a contact force applied only along the $\hat{\boldsymbol{t}}_1$ direction.

Table 28.10 Dimensions of the main subspaces and classifications of the grasp given in Example 3

Dimension	Class
dim $\mathcal{N}(\boldsymbol{J}^\top) = 6$	Defective
dim $\mathcal{N}(\boldsymbol{G}) = 3$	Graspable
dim $\mathcal{N}(\boldsymbol{J}^\top) \cap \mathcal{N}(\boldsymbol{G}) = 1$	Hyperstatic

The system is graspable because the subspace of internal forces is three dimensional; a possible basis matrix is:

$$N(\boldsymbol{G}) = \begin{pmatrix} 1 & 1 & 0 \\ 1 & 0 & 1 \\ 0 & 0 & 0 \\ \hline 1 & 0 & 2 \\ -1 & 0 & 0 \\ 0 & 0 & 0 \\ \hline 0 & 1 & 0 \\ 0 & 0 & -1 \\ 0 & 0 & 0 \end{pmatrix} .$$

The three force vectors of the subspace $N(\boldsymbol{G})$ are easily identified from Fig. 28.15. Note that all forces are expressed in local contact frames. The first column vector of $N(\boldsymbol{G})$ represents opposed forces at contacts 1 and 2 along the line joining contacts 1 and 2. The second column vector parameterizes opposed forces at contacts 1 and 3 along the line joining contacts 1 and 3. The last vector represents forces along direction $\boldsymbol{\lambda}_\mathrm{h}$, shown as the dashed lines in Fig. 28.15. Note that this direction (in wrench intensity space) corresponds to two upward friction forces at the left and right contacts and one downward with double the magnitude from the center of the top link in the work space.

Finally, the grasp is hyperstatic because

$$N(\boldsymbol{G}) \cap N(\boldsymbol{J}^\top) = \begin{pmatrix} 0 \\ 1 \\ 0 \\ \hline 2 \\ 0 \\ 0 \\ \hline 0 \\ -1 \\ 0 \end{pmatrix} \neq 0 .$$

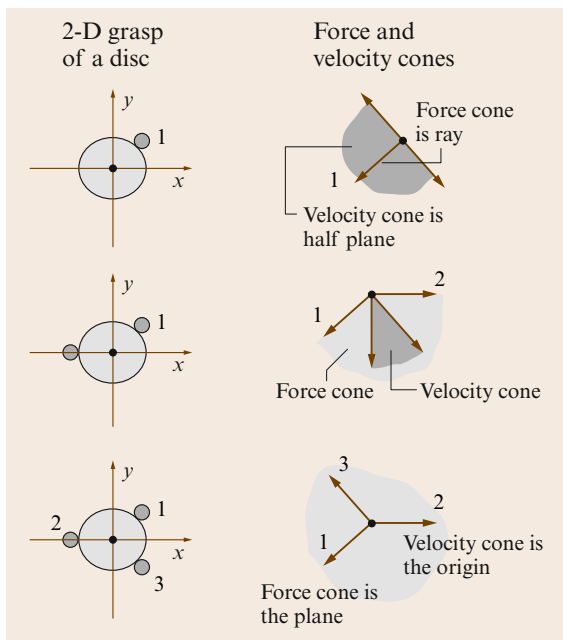Hyperstatic forces in this subspace are internal forces that cannot be controlled through the hand joints. In

Fig. 28.16 The case of a translating disc in the plane: relationship between frictionless contacts and possible disc velocities and net contact forces

Fig. 28.15 the internal force λ_h that is also in $N(J^\top)$ is reported.

The grasp in Fig. 28.15 is an example of a *power grasp*, a style of grasp mentioned earlier that uses many contact points not only on the fingertips but also on the links of fingers and the palm [28.4, 20, 31].

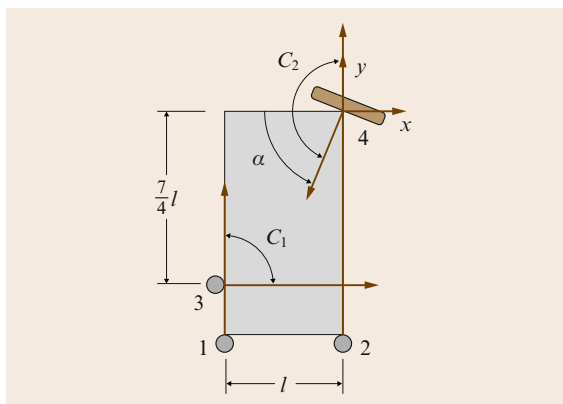All power grasps are kinematically defective ($\mathcal{N}(J^\top) \neq 0$) and are usually hyperstatic. According to Sect. 28.4.2, rigid-body modeling is not sufficient to capture the overall system behavior, because the generalized contact forces in $\mathcal{N}(G) \cap \mathcal{N}(J^\top)$ leave the dynamics indeterminate.

Many approaches have been used to overcome the rigid-body limitation in hyperstatic grasps such as those proposed in [28.12, 16, 17] where viscoelastic contact models have been used to solve the force indeterminacy. In [28.32], the authors found that a sufficient condition for hyperstaticity is $m > q + 6$, where m is the dimension of the contact force vector.

28.5.4 Example 4: Duality

Consider a frictionless disc constrained to translate in the plane (Fig. 28.16). In this problem $n_v = 2$, so the space of applied contact forces and object velocities is the plane $\mathbb{R}^2$. In the top pair of pictures, a single (fixed) contact point imposes a half-space constraint on the instantaneous velocity and limits the force at a frictionless contact to the ray. Both the ray and the (dark gray) half space are defined by the contact normal pointing into the object. Notice that the ray and half space are dual cones. When two contacts are present, the (light gray) force cone becomes the nonnegative span of the two contact normals and the velocity cone is its dual. With the addition of the third contact, the grasp has form closure, as indicated by the degeneration of the velocity cone to the origin and the expansion of the force cone to become equal to the plane.
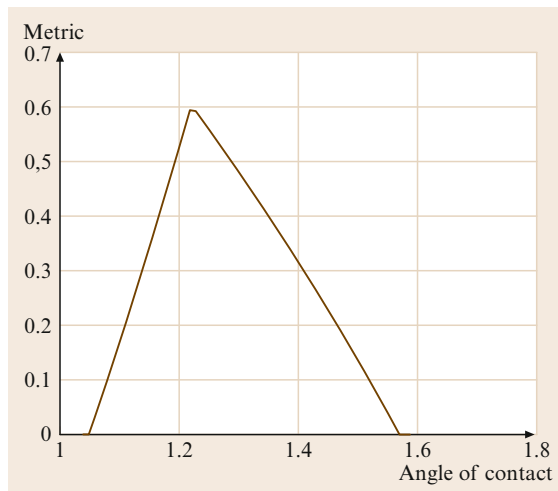

Fig. 28.17 Planar grasp with first-order form closure if $1.052 < \alpha < \frac{\pi}{2}$

Fig. 28.18 Plot of closure metric versus angle of contact if $1.04 < \alpha < 1.59$

It is important to point out that the discussion of the dual cones applies to three-dimensional bodies after replacing the contact normals with the columns of G.

28.5.5 Example 5: Form Closure

Form closure of a spatial object requires seven contacts, which is difficult to illustrate. Therefore, the only form closure example analyzed in this chapter is for the following planar problem.

The fundamental features of a planar grasp with four contacts are shown in Fig. 28.17. Notice that the normal at the fourth contact is well defined despite the contact occurring on the vertex of the object. The angle α of the finger is allowed to vary, and it can be shown that form

closure exists if α lies in the interval $1.0518 < \alpha < \frac{\pi}{2}$. Notice that a critical value of α occurs when the lower edge of $\mathcal{C}_2$ contains contact point 3 ($\alpha \approx 1.0518$) and contact point 2 ($\alpha = \frac{\pi}{2}$).

Choosing the frame for analysis with origin at the fourth contact point, the grasp matrix for this example is

$$ G = \begin{pmatrix} 0 & 0 & 1 & -\cos(\alpha) \\ 1 & 1 & 0 & -\sin(\alpha) \\ -l & 0 & \frac{7}{4}l & 0 \end{pmatrix} . \qquad (28.79) $$

Form closure was tested for a range of angles as shown in the plot in Fig. 28.18, which indicates that the grasp farthest from losing form closure has $\alpha \approx 1.22$ radians, which is the configuration shown in the figure.

28.6 Conclusion and Further Reading

A great deal of understanding of grasping systems can be derived from the simple linear kinematic, dynamic, and contact models. The most widely used grasp classifications and closure properties can all be derived from these models under the rigid-body assumption. Linearizing these models leads to metrics and tests that can be computed efficiently using computational linear algebra and linear programming techniques. In-depth discussions of grasp kinematics and grasp classification can be found in [28.11, 16, 21, 32–36]. When making simplifying assumptions, one has to wonder what insights have been lost. For the interested reader, there are a host of papers that analyze grasping system under more sophisticated assumptions. In general, bodies are curved and compliant [28.13, 22, 31, 37–39]. Contact friction models are not quite as simple as the Coulomb approximation so widely adopted, and presented in this chapter; for example, if a contact has to resist a moment about its normal, its effective tangential friction coefficient is reduced [28.29]. In our analysis, the quadratic Coulomb friction cone was approximated by a polyhedral cone. The analysis problems are more difficult when using the quadratic cone, but they are quite tractable [28.30, 40]. In principle, a properly designed hand–object system could be controlled to maintain all contacts, but worldly realities can lead to unwanted slipping or twisting.

Other important research topics within the area of grasping are: grasp synthesis, force distribution, stability, and dexterous manipulation. Grasp synthesis is the problem of choosing the posture of the hand and contact point locations to optimize a grasp quality metric. Note that this is quite a different issue from *grasp*

acquisition, which refers to the act of achieving the chosen grasp. Grasp acquisition is an act of dexterous manipulation. One of the first studies of grasp synthesis for multifingered hands was undertaken by *Jameson* in 1985 [28.41] who designed a Levenberg–Marquardt algorithm to search the surface of an object for the locations of three points that would achieve force closure. Since this work, many other metrics and approaches to searching for high-quality grasps have been implemented (see, for example, [28.42–47]). A recent paper by *Liu* et al. provides an in-depth discussion of several quality metrics. They further demonstrate that, if one chooses finger contact locations by optimizing the metrics and if a force closure grasp exists, then the grasps obtained are force closed [28.48]. For grasping of several objects simultaneously, see [28.49].

The grasp force distribution problem is that of finding *good* joint actions and contact forces to balance a given external load applied to the object. This problem was studied in the context of walking machines first by *McGhee* and *Orin* [28.50] and later by several others [28.51, 52]. Kumar and Waldron applied similar techniques to force distribution problems in grasping [28.53]. Recent work by *Han* et al. and *Buss* et al. has solved the force distribution problem with nonlinear friction cone constraints by taking advantage of second-order cone programming and related techniques [28.30, 40, 54]. In power grasps, this problem is more involved because contact forces that cannot be applied may exist, as studied in [28.17, 19, 20, 55].

Grasp stability is too often equated to grasp closure, because all external forces can be balanced by the hand.

However, grasp closure is really equivalent to the existence of equilibrium, which is a necessary condition for stability, but not a sufficient condition. The common definition of stability outside of the field of robotic grasping requires that, when a system is deflected from an equilibrium point, the system returns to this point. This was the approach taken by *Hanafusa* and *Asada*, who studied grasp stability for a hand with three elastic fingers [28.56]. *Cutkosky* took the analysis to three dimensions and accounted for finger and object curvatures [28.37]. He showed that stability was dependent on the stiffnesses of the fingers and controller and on the curvatures of the bodies in contact.

Dexterous manipulation research first appeared in the literature in the 1970s. *Hanafusa* and *Asada* developed a plan to turn a nut onto a bolt [28.57]. Since then a progression of increasingly complex manipulation tasks have been studied at varying degrees of detail. *Mason* and many of his students studied pushing tasks in the horizontal plane, see for example [28.58–61]. Other notable planar work can be found in [28.62–66]. The planning and execution of dexterous manipulation tasks in three dimensions continues to be an open problem in robotics. However, for several interesting approaches and many useful insights, the following reading is recommended [28.67–72].

References

28.1 J.K. Salisbury: Kinematic and Force Analysis of Articulated Hands. Ph.D. Thesis (Stanford University, Stanford 1982)

28.2 A.T. Miller, P.K. Allen: GraspIt! A versatile simulator for robotic grasping, IEEE Robot. Autom. Mag. **11**(4), 110–122 (2004)

28.3 A. Bicchi: Hands for dextrous manipulation and powerful grasping: A difficult road towards simplicity, IEEE Trans. Robot. Autom. **16**, 652–662 (2000)

28.4 K. Salisbury, W. Townsend, B. Ebrman, D. DiPietro: Preliminary design of a whole-arm manipulation system (WAMS), Proc. IEEE Int. Conf. Robot. Autom. (1988) pp. 254–260

28.5 M.S. Ohwovoriole, B. Roth: An extension of screw theory, J. Mech. Des. **103**, 725–735 (1981)

28.6 K.H. Hunt: *Kinematic Geometry of Mechanisms* (Oxford Univ. Press, Oxford 1978)

28.7 T.R. Kane, D.A. Levinson, P.W. Likins: *Spacecraft Dynamics* (McGraw Hill, New York 1980)

28.8 J.J. Craig: *Introduction to Robotics: Mechanics and Control*, 2nd edn. (Addison-Wesley, Reading 1989)

28.9 J.K. Salisbury, B. Roth: Kinematic and force analysis of articulated mechanical hands, J. Mech. Trans. Autom. Des. **105**, 35–41 (1983)

28.10 M.T. Mason, J.K. Salisbury Jr: *Robot Hands and the Mechanics of Manipulation* (MIT Press, Cambridge 1985)

28.11 A. Bicchi: On the closure properties of robotic grasping, Int. J. Robot. Res. **14**(4), 319–334 (1995)

28.12 D. Prattichizzo, A. Bicchi: Consistent task specification for manipulation systems with general kinematics, ASME J. Dyn. Syst. Meas. Contr. **119**, 760–767 (1997)

28.13 J. Kerr, B. Roth: Analysis of multifingered hands, Int. J. Robot. Res. **4**(4), 3–17 (1986)

28.14 G. Strang: *Introduction to Linear Algebra* (Wellesley-Cambridge, Wellesley 1993)

28.15 R.M. Murray, Z. Li, S.S. Sastry: A Mathematical Introduction to Robot Manipulation (CRC Press, Boca Raton 1993)

28.16 D. Prattichizzo, A. Bicchi: Dynamic analysis of mobility and graspability of general manipulation systems, IEEE Trans. Robot. Autom. **14**(2), 241–258 (1998)

28.17 A. Bicchi: On the problem of decomposing grasp and manipulation forces in multiple whole-limb manipulation, Int. J. Robot. Autom. Syst. **13**, 127–147 (1994)

28.18 F. Reuleaux: *The Kinematics of Machinery* (Macmillan, New York 1876), Republished by Dover, New York (1963)

28.19 T. Omata, K. Nagata: Rigid body analysis of the indeterminate grasp force in power grasps, IEEE Trans. Robot. Autom. **16**(1), 46–54 (2000)

28.20 J.C. Trinkle: The Mechanics and Planning of Enveloping Grasps. Ph.D. Thesis (University of Pennsylvania, Philadelphia 1987)

28.21 K. Lakshminarayana: Mechanics of form closure, Amer. Soc. Mech. Eng. Tech. Rep. **78-DET-32** (1978)

28.22 E. Rimon, J. Burdick: Mobility of bodies in contact i: A 2nd order mobility index for multiple-finger grasps, IEEE Trans. Robot. Autom. **14**(5), 696–708 (1998)

28.23 B. Mishra, J.T. Schwartz, M. Sharir: On the existence and synthesis of multifinger positive grips, Algorithmica **2**(4), 541–558 (1987)

28.24 P. Somov: Über Schraubengeschwindigkeiten eines festen Körpers bei verschiedener Zahl von Stützflächen, Z. Math. Phys. **42**, 133–153 (1897), (in German)

28.25 A.J. Goldman, A.W. Tucker: Polyhedral convex cones. In: *Linear Inequalities and Related Systems*, ed. by H.W. Kuhn, A.W. Tucker (Princeton Univ., York 1956) pp. 19–40

28.26 X. Markenscoff, L. Ni, C.H. Papadimitriou: The geometry of grasping, Int. J. Robot. Res. **9**(1), 61–74 (1990)

28.27 D.G. Luenberger: *Linear and Nonlinear Programming*, 2nd edn. (Addison-Wesley, Reading 1984)

28.28 V.D. Nguyen: The synthesis of force closure grasps in the plane. M.S. Thesis (MIT, Cambridge 1985), AI-TR861

28.29 R.D. Howe, M.R. Cutkosky: Practical force-motion models for sliding manipulation, Int. J. Robot. Res. **15**(6), 557–572 (1996)

28.30 L. Han, J.C. Trinkle, Z. Li: Grasp analysis as linear matrix inequality problems, IEEE Trans. Robot. Autom. **16**(6), 663–674 (2000)

28.31 M.R. Cutkosky, I. Kao: Computing and controlling the compliance of a robotic hand, IEEE Trans. Robot. Autom. **5**(2), 151–165 (1989)

28.32 J.C. Trinkle: On the stability and instantaneous velocity of grasped frictionless objects, IEEE Trans. Robot. Autom. **8**(5), 560–572 (1992)

28.33 K.H. Hunt, A.E. Samuel, P.R. McAree: Special configurations of multi-finger multi-freedom grippers – a kinematic study, Int. J. Robot. Res. **10**(2), 123–134 (1991)

28.34 D.J. Montana: The kinematics of multi-fingered manipulation, IEEE Trans. Robot. Autom. **11**(4), 491–503 (1995)

28.35 Y. Nakamura, K. Nagai, T. Yoshikawa: Passive and active closures by constraining mechanisms, Int. J. Robot. Res. **8**, 44–61 (1989)

28.36 J.S. Pang, J.C. Trinkle: Stability characterizations of rigid body contact problems with coulomb friction, Z. Angew. Math. Mech. **80**(10), 643–663 (2000)

28.37 M.R. Cutkosky: *Robotic Grasping and Fine Manipulation* (Kluwer Academic, Norwell 1985)

28.38 W.S. Howard, V. Kumar: On the stability of grasped objects, IEEE Trans. Robot. Autom. **12**(6), 904–917 (1996)

28.39 A.B.A. Cole, J.E. Hauser, S.S. Sastry: Kinematics and control of multifingered hands with rolling contacts, IEEE Trans. Autom. Contr. **34**, 398–404 (1989)

28.40 M. Buss, H. Hashimoto, J. Moore: Dexterous hand grasping force optimization, IEEE Trans. Robot. Autom. **12**(3), 406–418 (1996)

28.41 J. Jameson: Analytic Techniques for Automated Grasp. Ph.D. Thesis (Stanford University, Stanford 1985)

28.42 V. Nguyen: Constructing force-closure grasps, Int. J. Robot. Res. **7**(3), 3–16 (1988)

28.43 N.S. Pollard: Parallel algorithms for synthesis of whole-hand grasps, Proc. IEEE Int. Conf. Robot. Autom. (1997)

28.44 Y.C. Park, G.P. Starr: Grasp synthesis of polygonal objects using a three-fingered robot hand, Int. J. Robot. Res. **11**(3), 163–184 (1992)

28.45 I.M. Chen, J.W. Burdick: Finding antipodal point grasps on irregularly shaped objects, IEEE Trans. Robot. Autom. **9**(4), 507–512 (1993)

28.46 B. Mishra: Grasp metrics: Optimality and complexity, Proc. Workshop Algorithmic Found. Robot. (Peters, Boston 1994)

28.47 J. Ponce, S. Sullivan, A. Sudsang, J.-D. Boissonnat, J.-P. Merlet: On computing four-finger equilibrium and force-closure grasps of polyhedral objects, Int. J. Robot. Res. **16**(1), 11–35 (1997)

28.48 G.F. Liu, J. Xu, X. Wang, Z.X. Li: On quality functions for grasp synthesis, fixture planning, and coordinated manipulation, IEEE Trans. Autom. Sci. Eng. **1**(2), 146–162 (2004)

28.49 K. Harada, M. Kaneko: Neighborhood equilibrium grasp for multiple objects, Proc. IEEE Int. Conf. Robot. Autom. (2000) pp. 2159–2164

28.50 R.B. McGhee, D.E. Orin: A mathematical programming approach to control of positions and torques in legged locomotion systems, Proc. RO-MANCY (1976)

28.51 K. Waldron: Force and motion management in legged locomotion, IEEE J. Robot. Autom. **2**(4), 214–220 (1986)

28.52 T. Yoshikawa, K. Nagai: Manipulating and grasping forces in manipulation by multi-fingered grippers, Proc. IEEE Int. Conf. Robot. Autom. (1987) pp. 1998–2007

28.53 V. Kumar, K. Waldron: Force distribution in closed kinematic chains, IEEE J. Robot. Autom. **4**(6), 657–664 (1988)

28.54 M. Buss, L. Faybusovich, J. Moore: Dikin-type algorithms for dexterous grasping force optimization, Int. J. Robot. Res. **17**(8), 831–839 (1998)

28.55 D. Prattichizzo, J.K. Salisbury, A. Bicchi: Contact and grasp robustness measures: Analysis and experiments. In: *Experimental Robotics IV*, Lecture Notes Contr. Inf. Sci., Vol. 223, ed. by O. Khatib, K. Salisbury (Springer, Berlin, Heidelberg 1997)

28.56 H. Hanafusa, H. Asada: Stable prehension by a robot hand with elastic fingers. In: *Robot Motion: Planning and Control*, ed. by M. Brady, J. Hollerbach, T. Johnson, T. Lozano-Perez, M. Mason (MIT Press, Cambridge 1982) pp. 323–336

28.57 H. Hanafusa, H. Asada: Handling of constrained objects by active elastic fingers and its applications to assembly, Trans. Soc. Instrum. Contr. Eng. **15**(1), 61–66 (1979)

28.58 M.T. Mason: Manipulator Grasping and Pushing Operations. Ph.D. Thesis (Massachusetts Institute of Technology, Cambridge 1982), reprinted in *Robot Hands and the Mechanics of Manipulation* MIT Press, Cambridge 1985

28.59 R.C. Brost: Analysis and Planning of Planar Manipulation Tasks. Ph.D. Thesis (Carnegie Mellon University, Pittsburgh 1991)

28.60 M.A. Peshkin, A.C. Sanderson: Planning robotic manipulation strategies for workpieces that slide, IEEE J. Robot. Autom. **4**(5), 524–531 (1988)

Part D | 28

28.61   K. Lynch: Nonprehensile Manipulation: Mechanics and Planning. Ph.D. Thesis (Carnegie Mellon University, Pittsburgh 1996)

28.62   J.C. Trinkle, J.J. Hunter: A framework for planning dexterous manipulation, Proc. IEEE Int. Conf. Robot. Autom. (1991) pp. 1245–1251

28.63   J.C. Trinkle, R.C. Ram, A.O. Farahat, P.F. Stiller: Dexterous manipulation planning and execution of an enveloped slippery workpiece, Proc. IEEE Int. Conf. Robot. Autom., Vol. 2 (1993) pp. 442–448

28.64   K. Harada, M. Kaneko, T. Tsuji: Rolling based manipulation for multiple objects, Proc. IEEE Int. Conf. Robot. Autom. (2000) pp. 3887–3894

28.65   R.S. Fearing: Simplified grasping and manipulation with dextrous robot hands, IEEE J. Robot. Autom. **RA-2**(4), 188–195 (1986)

28.66   N.B. Zumel, M.A. Erdmann: Nonprehensible two palm manipulation with non-equilbrium transitions between stable states, Proc. IEEE Int. Conf. Robot. Autom. (1996) pp. 3317–3323

28.67   D.L. Brock: Enhancing the dexterity of a robot hand using controlled slip. M.S. Thesis (MIT, Cambridge 1987)

28.68   R. Fearing, S. Gopalswamy: Grasping polyhedral objects with slip, Proc. IEEE Int. Conf. Robot. Autom. (1989) pp. 296–301

28.69   M. Cherif, K.K. Gupta: Planning quasi-static fingertip manipulation for reconfiguring objects, IEEE Trans. Robot. Autom. **15**(5), 837–848 (1999)

28.70   L. Han, J.C. Trinkle: Dextrous manipulation by rolling and finger gaiting, Proc. IEEE Int. Conf. Robot. Autom. (1998) pp. 730–735

28.71   L. Han, Z. Li, J.C. Trinkle, Z. Qin, S. Jiang: The planning and control of robot dexterous manipulation, Proc. IEEE Int. Conf. Robot. Autom. (2000) pp. 263–269

28.72   M. Higashimori, M. Kimura, I. Ishii, M. Kaneko: Friction independent dynamic capturing strategy for a 2d stick-shaped object, Proc. IEEE Int. Conf. Robot. Autom. (2007) pp. 217–224